Published in final edited form as:
Neuron. 2012 May 24; 74(4): 676–690. doi:10.1016/j.neuron.2012.03.025.

Optic chiasm presentation of Semaphorin6D in the context of Plexin-A1 and Nr-CAM promotes retinal axon midline crossing

Takaaki Kuwajima[1], **Yutaka Yoshida**[3,4], **Noriko Takegahara**[5,6], **Timothy J. Petros**[1,7], **Atsushi Kumanogoh**[5], **Thomas M. Jessell**[3], **Takeshi Sakurai**[8,9], and **Carol Mason**[1,2]

[1]Departments of Pathology and Cell Biology, and Neuroscience, College of Physicians and Surgeons, Columbia University, New York, New York 10032

[2]Department of Ophthalmology, College of Physicians and Surgeons, Columbia University, New York, New York 10032

[3]Howard Hughes Medical Institute, Kavli Institute for Brain Science, Departments of Neuroscience, and Biochemistry and Molecular Biophysics, College of Physicians and Surgeons, Columbia University, New York, NY 10032, USA

[5]Department of Immunopathology, Immunology Frontier Research Center (iFReC), Research Institute for Microbial Diseases, Osaka University, 3-1 Yamadaoka, Suita, Osaka 565-0871, Japan

[8]Departments of Psychiatry, Pharmacology and Systems Therapeutics, Black Family Stem Cell Institute, Mount Sinai School of Medicine, New York, New York 10029, USA

Summary

At the optic chiasm, retinal ganglion cells (RGCs) project ipsi- or contralaterally to establish the circuitry for binocular vision. Ipsilateral guidance programs have been characterized, but contralateral guidance programs are not well understood. Here we identify a tripartite molecular system for contralateral RGC projections: Semaphorin 6D and Nr-CAM are expressed on midline radial glia and Plexin-A1 on chiasm neurons, and Plexin-A1 and Nr-CAM are also expressed on contralateral RGCs. Sema6D is repulsive to contralateral RGCs, but Sema6D in combination with Nr-CAM and Plexin-A1 converts repulsion to growth-promotion. Nr-CAM functions as a novel receptor for Sema6D. Sema6D, Plexin-A1 and Nr-CAM are all required for efficient RGC decussation at the optic chiasm. These findings suggest a novel mechanism by which a complex of Sema6D, Nr-CAM, and Plexin-A1 at the chiasm midline alters the sign of Sema6D and signals Nr-CAM/Plexin-A1 receptors on RGCs to implement the contralateral RGC projection.

[4]Present address: Division of Developmental Biology, Cincinnati Children's Hospital Medical Center, Cincinnati, Ohio 45229, USA
[6]Present address: Department of Pathology and Laboratory Medicine, University of Pennsylvania School of Medicine, Philadelphia, PA 19104
[7]Present address: Department of Psychiatry, Weill Cornell Medical College, New York, NY 10021
[9]Present address: Medical Innovation Center, Graduate School of Medicine, Kyoto University, Yoshidakonoe-cho, Sakyo-ku, Kyoto 606-8501, Japan

Introduction

Along the rostro-caudal extent of the neuraxis, neurons decide whether to traverse or avoid the midline - a fundamental decision that is crucial for the bilateral coordination of neural circuits. In higher vertebrates, two major classes of retinal ganglion cell (RGC) axons converge at the ventral diencephalon midline to form the optic chiasm. RGCs arising from the temporal retina (in mouse, the ventrotemporal (VT) crescent) project ipsilaterally, whereas RGCs from nasal retina (in mouse, all other retinal regions outside of the VT crescent or, non-VT) project contralaterally. Axonal decussation establishes the basic circuit for binocular vision (Erskine and Herrera, 2007; Guillery et al., 1995; Petros et al., 2008), but the molecular mechanisms that direct RGC divergence at the optic chiasm midline remain elusive.

Soon after RGC axons exit the optic stalk, they encounter guidance cues expressed by radial glial cells at the optic chiasm midline as well as by midline neurons situated caudal to the chiasm (Mason and Sretavan, 1997; Petros et al., 2008). In contrast to non-VT RGC neurites ipsilateral RGCs from VT retina extend shorter neurites on chiasm cells *in vitro,* (Petros et al., 2009; Wang et al., 1995; Williams et al., 2003), implicating a repulsive cue at the midline that directs VT RGC axons ipsilaterally. The molecular program for the ipsilateral (uncrossed) retinal projection involves Ephrin-B2 ligand expressed on radial glial cells at the chiasm midline which repels EphB1-positive VT RGC growth cones (Nakagawa et al., 2000; Petros et al., 2010; Williams et al., 2003). The ipsilateral trajectory and EphB1 expression is regulated by selective expression of the transcription factor Zic2 in those RGCs that fail to cross the chiasm midline (Garcia-Frigola et al., 2008; Herrera et al., 2003; Lee et al., 2008; Petros et al., 2009).

How the crossed RGC axonal projection is established remains unclear. The crossed pathway could form passively with crossed RGC axons lacking receptors to respond to inhibitory chiasmatic cues and thus projecting across the midline by default (Guillery et al., 1995). Alternatively, attractive and/or growth supporting factors could facilitate midline crossing by luring RGCs toward and through the midline, as in the ventral midline of the spinal cord (Dickson and Zou, 2010). A third possibility is that RGCs with a contralateral trajectory have acquired the ability to overcome an intrinsically inhibitory chiasm environment.

We previously identified Ng-CAM-related cell adhesion molecule (Nr-CAM) as a candidate molecule that facilitates RGC chiasm crossing. Nr-CAM is expressed by non-VT RGCs and by radial glial cells at the chiasm midline. Nr-CAM is also expressed in late-born RGCs that settle in the VT region and project contralaterally. *In vivo*, Nr-CAM is important only for the late-born contralateral projection from the VT crescent (Williams et al., 2006). Presumably other factors function alone or in concert with Nr-CAM to mediate midline crossing, to support the growth of contralaterally-projecting RGC axons, and/or to overcome inhibition at the midline. Members of the L1 family of cell adhesion molecules (CAMs), notably Nr-CAM, interact with Semaphorins (Semas) and have been suggested to play a role in midline crossing (Bechara et al., 2007; Derijck et al., 2010; Niquille et al., 2009; Piper et al., 2009; Sakai and Halloran, 2006).

We have considered the possibility that Semas and their receptors might partner with Nr-CAM to regulate midline crossing at the mouse optic chiasm. We show here that a tripartite molecular system directs contralateral RGC axons across the optic chiasm midline. Nr-CAM and Semaphorin6D (Sema6D) are expressed on radial glia, Plexin-A1 is expressed on neurons around the chiasm midline, and Plexin-A1 and Nr-CAM are expressed on contralateral RGC axons. Alone, the unconstrained actions of Sema6D repel RGCs with a

crossed projection, but presentation of Sema6D in combination with Nr-CAM and Plexin-A1 promotes rather than repels axonal growth of crossed RGCs. We also show that Nr-CAM functions as an axonal receptor for Sema6D, and that Sema6D, Plexin-A1 and Nr-CAM are each required for efficient RGC decussation at the optic chiasm *in vivo*. These findings suggest that contralateral projections depend on the expression of Sema6D, Nr-CAM and Plexin-A1 by midline chiasm cells – forming a ligand complex that activates a Nr-CAM/Plexin-A1 receptor system on RGCs.

Results

Sema6D and Plexin-A1 are expressed in the optic chiasm

Several lines of evidence prompted us to investigate the expression patterns of semaphorins at the optic chiasm. First, semaphorins are involved in a variety of midline models (Derijck et al., 2010; Piper et al., 2009; Sakai and Halloran, 2006). Second, Ig-CAMs are known to modulate semaphorin signaling (Bechara et al., 2007; Nawabi et al., 2010; Wolman et al., 2007). We therefore examined the expression pattern of semaphorins in the retina and optic chiasm, initially focusing on semaphorin3 (Sema3) and semaphorin6 (Sema6) family members because of their established roles in axon guidance in the mouse forebrain and spinal cord (Derijck et al., 2010; Pecho-Vrieseling et al., 2009; Piper et al., 2009; Runker et al., 2008; Suto et al., 2005; Yoshida et al., 2006).

We identified Sema6D mRNA enriched in the chiasm in the rostral and middle sectors of the chiasm midline, similar to Nr-CAM (Lustig et al., 2001; Williams et al., 2006) (Figure 1A). Sema6D colocalizes with Nr-CAM in $RC2^+$ radial glia at the chiasm midline from E13.5–E17.5 (Figures 1B and 1C), although Sema6D expression extends dorsally along the ventricular zone of the third ventricle (Figure 1A). In the retina, Sema6D is restricted to the optic disc, resembling the expression pattern of EphA4 in glial cells at the optic nerve head (Petros et al., 2006) (Figure S1A). Sema6A and 6C are expressed in the region dorsal and lateral to the supraoptic area of the ventral diencephalon, and thus are not candidates for regulating midline crossing (Figure S1A). Sema3A, B and D mRNAs are not expressed at the chiasm midline (Figure S1A).

The only known receptors for Sema6D are Plexin-A1 and Plexin-A4, and these receptors can function in axon guidance independent of neuropilins (Takegahara et al., 2006; Toyofuku et al., 2004; Yoshida et al., 2006). Plexin-A1 is expressed in the $CD44^+/SSEA\text{-}1^+$ early born neurons caudal to the chiasm and in two oval groups of $SSEA\text{-}1^-$ cells caudal and slightly dorsal to the chiasm (Figure S1C). A raphe of $Plexin\text{-}A1^+/SSEA\text{-}1^+$ neurons extends between the palisade of $Nr\text{-}CAM^+/Sema6D^+$ radial glia that expresses $Nr\text{-}CAM^+/Sema6D^+$ (Figure 1D).

In summary, Sema6D is expressed in $Nr\text{-}CAM^+$ radial glia at the chiasm midline, and its receptor Plexin-A1 is expressed in the $CD44^+/SSEA\text{-}1^+$ neurons caudal to and intersecting the chiasm radial glia (Figure 1E). These expression patterns raise the possibility that Sema6D, Plexin-A1 and Nr-CAM might be involved in guiding RGCs across the chiasm midline.

Sema6D inhibits crossed RGC axons but promotes axonal outgrowth in the context of the optic chiasm

To identify the potential contribution of Sema6D in RGC divergence at the optic chiasm, we made use of our *in vitro* culture assay of uncrossed ventrotemporal (VT) or crossed dorsotemporal (DT) retinal explants on dissociated chiasm cells (Figure S2A). In dissociated chiasm cell cultures, 50.6% of cultured chiasm cells are $RC2^+$ cells, almost all of which express both Sema6D and Nr-CAM, and 36.7% of cells are $SSEA\text{-}1^+$ neurons, almost all of

which express Plexin-A1 (data not shown). Axons from both DT and VT explants grow extensively on laminin substrates. When grown on chiasm cells, neurite outgrowth from VT explants was reduced by 68% whereas DT explant neurite outgrowth was reduced only by 25% (DT + Chiasm = 0.75±0.02 versus VT + Chiasm = 0.30±0.02, $p<0.01$) (Figures S2B and S2C). Thus, on chiasm cells, crossed RGCs extend longer neurites than uncrossed RGCs, reflecting their differential behavior at the midline *in vivo*. Nonetheless, neurite outgrowth from crossed RGCs is moderately decreased on chiasm cells, suggesting the presence of inhibitory factors intrinsic to chiasm cells that dampen the growth of crossed RGCs and must be overcome during RGC traverse of the midline.

To investigate a role for Sema6D in RGC axon outgrowth, E14.5 DT or VT retinal explants were cocultured with dissociated chiasm cells (Figure S2) in the presence of a function-blocking Sema6D antibody (αSema6D) or a control antibody (αcontrol) (Figure S3). Whereas αSema6D had no effect on VT explant outgrowth, application of αSema6D significantly reduced DT explant neurite outgrowth on chiasm cells by 50% compared to cocultures with αcontrol (DT + Chiasm + αSema6D = 0.50±0.03 versus DT + Chiasm + αCtr = 1.02±0.05, $p<0.01$) (Figures 2A and 2B). These data support the hypothesis that Sema6D is important for growth of contralaterally-projecting RGCs at the chiasm midline.

To further test the effect of Sema6D on RGC outgrowth, we measured neurite growth from E14.5 DT and VT explants cultured on HEK cells expressing full length Sema6D (Figures 2C and 2D). We observed a 55% reduction in DT explant neurite outgrowth on Sema6D$^+$ HEK cells compared to explants growing on control HEK cells with vector alone (DT + HEK Sema6D + αCtr = 0.45±0.03 versus DT + HEK Ctr + αCtr = 1.0±0.03, $p<0.01$) (Figures 2C–2E). This reduction was attenuated by αSema6D, leading to a reduction of growth only to 10% of control values (Figures 2D and 2E) (DT + HEK Sema6D + αSema6D = 0.90±0.05 versus DT + HEK Sema6D + αCtr = 0.45±0.03, $p<0.01$). As in coculture with chiasm cells, VT explant neurite outgrowth on Sema6D$^+$ HEK cells was similar with or without αSema6D, indicating that uncrossed RGC axons do not respond to Sema6D (Figures 2D and 2E).

Thus, while Sema6D presented alone in HEK cells is inhibitory to crossed RGCs, Sema6D is important for RGC midline crossing in the context of the optic chiasm.

Nr-CAM and Plexin-A1 reverse the effect of Sema6D on crossed RGCs

The finding that Sema6D supports crossed RGC outgrowth on chiasm cells suggests that factors at the chiasm midline convert Sema6D from an inhibitory to a growth-promoting factor. Sema6D is coexpressed with Nr-CAM by radial glial cells at the chiasm midline, and Plexin-A1 is expressed by SSEA-1$^+$ chiasm neurons that extend into the chiasm midline (Figure 1E). We therefore considered whether Nr-CAM and/or Plexin-A1, in the context of the optic chiasm environment, modulate the repulsive effect of Sema6D on crossed axons.

Because HEK cells that are singly transfected do not fully recapitulate the cellular composition of the optic chiasm, we designed a HEK-retina coculture system to present Sema6D, Plexin-A1 and Nr-CAM in a manner that best mimics their expression in the different cell types at the optic chiasm *in vivo*: Sema6D and Nr-CAM were coexpressed in one set of HEK cells (to mimic radial glia cells) and Plexin-A1 was expressed in a separate population of HEK cells (to mimic SSEA-1$^+$ chiasm neurons). When DT explants were grown on Sema6D$^+$/Nr-CAM$^+$ HEK cells, or Sema6D$^+$ HEK cells mixed with Plexin-A1$^+$ HEK cells, neurite outgrowth was significantly improved compared to explants grown on Sema6D$^+$ HEK cells (DT + HEK Sema6D/ Nr-CAM = 0.76±0.05 and DT + HEK Sema6D + HEK Plexin-A1 = 0.71±0.02 versus DT + HEK Sema6D = 0.58±0.01 and DT + HEK Ctr = 1.0±0.02, $p<0.01$) (Figure 3A). Strikingly, however, when retinal explants were plated on

a combination of Sema6D$^+$/Nr-CAM$^+$ HEK cells and Plexin-A1$^+$ HEK cells, DT RGC outgrowth was increased by ~40% over control levels (DT + HEK Sema6D/Nr-CAM + HEK Plexin-A1 = 1.40±0.02 versus DT + HEK Ctr = 1.0±0.02, p<0.01) (Figures 3A). Further, when retinal explants were plated on Sema6D$^+$/Nr-CAM$^+$ HEK cells and GST-Plexin-A1 ectodomain protein added, DT RGC outgrowth was increased to an even greater extent, by ~70% over control levels (Figure 3B). Thus, the configuration of HEK cells that best mimics the *in vivo* chiasm scenario (Sema6D$^+$/Nr-CAM$^+$ HEK cells + Plexin-A1$^+$ HEK cells or Sema6D$^+$/Nr-CAM$^+$ HEK cells + Plexin-A1 ectodomain) leads to a switch of repulsion by Sema6D to growth-promotion of DT retinal neurites (Figure 3C). The ectodomain experiments emphasize that Plexin-A1 must work in *trans* to overcome the repulsive effects of Sema6D.

To further test a role for chiasm Sema6D, Nr-CAM and Plexin-A1 in implementing RGC crossing, we plated retinal explants from WT embryos on chiasm cells from *Plexin-A1*$^{-/-}$, *Nr-CAM*$^{-/-}$, or *Plexin-A1*$^{-/-}$;*Nr-CAM*$^{-/-}$ double mutant mice (Figures 3D and 3E). WT DT axons extended less well on *Plexin-A1*$^{-/-}$ or *Nr-CAM*$^{-/-}$ chiasm cells compared to WT chiasm cells, and poorly on *Plexin-A1*$^{-/-}$;*Nr-CAM*$^{-/-}$ chiasm cells (60% reduction) (DT + DKO Chiasm = 0.40±0.01 versus DT + WT Chiasm = 1.0±0.02, p<0.01). The reduced outgrowth of WT DT explants on *Plexin-A1*$^{-/-}$;*Nr-CAM*$^{-/-}$ chiasm cells was ameliorated by addition of αSema6D (DT + DKO Chiasm + αSema6D = 0.86±0.03 versus DT + DKO Chiasm = 0.40±0.01. p<0.01), indicating that in the absence of chiasm cell-derived Plexin-A1 and Nr-CAM, chiasm cells are inhibitory to RGC axon growth due to the presence of Sema6D. These results suggest that within the chiasm environment, Nr-CAM and Plexin-A1, expressed in chiasmatic radial glia and SSEA-1$^+$ neurons, respectively, act to support RGC axon growth across the optic chiasm midline by modifying the effect of Sema6D on radial glia from a repulsive to a growth-promoting cue.

Plexin-A1 and Nr-CAM are expressed on crossed RGCs

If Sema6D is a cue that is involved in midline crossing, the only known receptors, Plexin-A1 and -A4 may be restricted to crossed uncrossed RGCs. By *in situ* hybridization and immunostaining, we established that Plexin-A1 is predominantly expressed in non-VT RGCs from E13–E17.5 and it is upregulated in E17.5 VT RGCs when late-born VT RGCs extend contralaterally (Williams et al., 2006) (Figures 4A and 4B). Plexin-A4 is not expressed in RGCs during these periods (Figure S1B). To verify that Plexin-A1 is expressed in crossed RGCs, we localized Plexin-A1 mRNA and Zic2, a transcription factor expressed only in VT RGCs at E14.5 (Herrera et al., 2003). Roughly 90% of Zic2$^+$ RGCs were Plexin-A1-negative. Some RGCs expressing both Zic2 and Plexin-A1 were positioned at the central border of the VT region (Figure 4C). Plexin-A1 protein is detectable on DT growth cones but not on WT VT or *Plexin-A1*$^{-/-}$ DT neurites (Figure 4D). Thus, similar to Nr-CAM, Plexin-A1 is expressed by RGCs with a crossed trajectory (Figure 4E).

Plexin-A1 and Nr-CAM on crossed RGCs mediate both repulsive and growth-promoting effects of Sema6D

To address whether Plexin-A1 and/or Nr-CAM on crossed RGCs are required for Sema6D-induced behaviors, we cultured E14.5 DT and VT explants from *Plexin-A1*$^{-/-}$, *Nr-CAM*$^{-/-}$, and *Plexin-A1*$^{-/-}$;*Nr-CAM*$^{-/-}$ retina on WT chiasm cells (Figures 5A and 5B). There was no significant difference in outgrowth of DT explants from WT, *Plexin-A1*$^{-/-}$, *Nr-CAM*$^{-/-}$ and *Plexin-A1*$^{-/-}$;*Nr-CAM*$^{-/-}$ retina on a laminin substrate (Figures S4A and S4B). Additionally, outgrowth from *Plexin-A1*$^{-/-}$;*Nr-CAM*$^{-/-}$ VT retinal explants was comparable to the growth from explants of WT VT retina (data not shown).

In contrast, neurite outgrowth from DT explants of *Plexin-A1*$^{-/-}$ and *Nr-CAM*$^{-/-}$ mutants was reduced on WT chiasm cells by 37% and 29%, respectively (Figures 5A and 5B). An even greater reduction in neurite outgrowth (64%) was observed in DT explants from *Plexin-A1*$^{-/-}$*;Nr-CAM*$^{-/-}$ retina, similar to the reduction of outgrowth of DT explants with chiasm cells in the presence of αSema6D (50% reduction) (WT DT + Chiasm = 1.0±0.03 versus *Plexin-A1*$^{-/-}$ DT + Chiasm = 0.63±0.01 P<0.01, *Nr-CAM*$^{-/-}$ DT + Chiasm = 0.71±0.003, p<0.01 and *Plexin-A1*$^{-/-}$*;Nr-CAM*$^{-/-}$ DT + Chiasm = 0.36±0.01, p<0.01) (Figure 2A). These findings suggest that expression of Plexin-A1 and Nr-CAM in DT RGCs is required to support outgrowth of crossed RGC axons on chiasm cells.

Next, we compared neurite outgrowth of DT retinal explants from WT, *Nr-CAM*$^{-/-}$, *Plexin-A1*$^{-/-}$ and *Plexin-A1*$^{-/-}$*;Nr-CAM*$^{-/-}$ retina on Sema6D^{+} HEK cells. There was no significant difference in the outgrowth of DT explants from WT, *Nr-CAM*$^{-/-}$, *Plexin-A1*$^{-/-}$ or *Plexin-A1*$^{-/-}$*;Nr-CAM*$^{-/-}$ on control HEK cells (Figure 5C). VT explants from *Nr-CAM*$^{-/-}$, *Plexin-A1*$^{-/-}$ and *Plexin-A1*$^{-/-}$*;Nr-CAM*$^{-/-}$ retina grew similarly on control and Sema6D^{+} HEK cells (Figures S4C and S4D). However, whereas WT DT neurite outgrowth on Sema6D^{+} HEK cells was reduced by 62%, neurite outgrowth from *Nr-CAM*$^{-/-}$ and *Plexin-A1*$^{-/-}$ DT explants was only mildly reduced, by 19% and 29%, respectively. Moreover, neurite outgrowth of DT explants from *Plexin-A1*$^{-/-}$*;Nr-CAM*$^{-/-}$ grown on Sema6D^{+} HEK cells was not reduced (WT DT + HEK Sema6D = 0.38±0.10 versus *Plexin-A1*$^{-/-}$ DT + HEK Sema6D = 0.81±0.02, p<0.01, *Nr-CAM*$^{-/-}$ DT + HEK Sema6D = 0.71±0.03, P<0.01 and *Plexin-A1*$^{-/-}$*;Nr-CAM*$^{-/-}$ DT + HEK Sema6D = 0.99±0.01, p<0.01) (Figure 5C). Thus, both Nr-CAM and Plexin-A1 expression by RGCs are required for Sema6D-elicited repulsion and for outgrowth on Sema6D^{+} chiasm cells.

To further explore the role of Plexin-A1 and Nr-CAM on RGCs for growth support in the context of the optic chiasm midline, we cocultured WT, *Nr-CAM*$^{-/-}$, *Plexin-A1*$^{-/-}$ or *Plexin-A1*$^{-/-}$*;Nr-CAM*$^{-/-}$ retinal explants on Sema6D^{+}/Nr-CAM^{+} and Plexin-A1^{+} HEK cells (mimicking the chiasm environment *in vivo*). WT DT RGC outgrowth was increased above control levels by 46% on a mixture of Sema6D^{+}/Nr-CAM^{+} and Plexin-A1^{+} HEK cells (WT DT + HEK Sema6D/Nr-CAM + HEK Plexin-A1 = 1.46±0.02 versus WT DT + HEK Ctr = 1.00±0.023, p<0.01) (Figure 5D; also see Figure 3A). The growth promoting effect of Nr-CAM^{+}/Sema6D^{+} and Plexin-A1^{+} HEK cells on WT DT explant neurites occurred to a lesser extent in DT explants from *Plexin-A1*$^{-/-}$ or *Nr-CAM*$^{-/-}$ retina (24% and 21% increase, respectively) (WT DT + HEK Ctr = 1.00±0.023 versus *Plexin-A1*$^{-/-}$ DT +HEK Sema6D/Nr-CAM + HEK Plexin-A1 = 1.24±0.04, p<0.01 and *Nr-CAM*$^{-/-}$ DT + HEK Sema6D/Nr-CAM + HEK Plexin-A1 = 1.21±0.02, p<0.01) and was not observed at all in *Plexin-A1*$^{-/-}$*;Nr-CAM*$^{-/-}$ DT explants (Figure 5D). Thus, both Plexin-A1 and Nr-CAM are required on crossed RGCs for inhibition by Sema6D alone and growth promotion by Sema6D presented together with Nr-CAM and Plexin-A1 (Figure 5E). Note that Plexin-A1 and Nr-CAM expressed on RGCs seem to play equivalent, additive roles in this function (Figures 5A, 5C and 5D).

The late-born crossed VT projection relies on Plexin-A1, Nr-CAM and Sema6D for midline crossing

At E17.5, Plexin-A1 and Nr-CAM are expressed in both non-VT and in VT retina (Figure 4B; (Williams et al., 2006). Sema6D is still expressed at the chiasm midline at E17.5 (Figure 1C). Consequently, both DT and VT WT explants from E17.5 retina cultured in the presence of αSema6D grew more poorly on chiasm cells compared to growth on chiasm cells without αSema6D (DT + Chiasm + αSema6D = 0.50±0.01 versus DT + Chiasm + αCtr = 0.69±0.01, p<0.01; VT + Chiasm + αSema6D = 0.27±0.01 versus VT + Chiasm + αCtr = 0.69±0.02, p<0.01) (Figure S7D). Thus, the late-born RGCs in VT retina that have a contralateral projection are responsive to Sema6D, corresponding to the late expression of

Plexin-A1 and Nr-CAM in the VT retina after E17.5, and further supporting the hypothesis that Plexin-A1 and Nr-CAM on crossed RGCs requires Sema6D, Plexin-A1 and Nr-CAM at the optic chiasm to implement midline crossing.

Nr-CAM is a receptor for Sema6D

To investigate whether Nr-CAM might directly interact with Sema6D, we examined the binding of Sema6D to Nr-CAM and other CAMs such as L1, Neurofascin and TAG-1, all of which are predominantly expressed in contralaterally-projecting RGCs *in vivo* (Bechara et al., 2007; Maness and Schachner, 2007; Williams et al., 2006) and on their axons and growth cones *in vitro* (Figure 6A). We performed an alkaline phosphatase (AP) binding assay by adding AP-Sema6D to HEK cells expressing Sema receptors or different CAMs (Yoshida et al., 2006). Sema6D binding was detected on Plexin-A1^{+} HEK cells, and also on Nr-CAM^{+} HEK cells, but not on cells expressing other Sema receptors including Neuropilin1 (expressed in RGCs, Figure S1B), or CAMs (Figure 6B). Nr-CAM-Sema6D binding was perturbed by αSema6D treatment (Figure S5A). In addition, using AP-Sema6C and AP-Sema6A, we found that Nr-CAM interacts with Sema6C but not Sema6A, highlighting some degree of specificity in Nr-CAM-Sema6D interactions (Figure S5A). Thus, Nr-CAM can bind to Sema6D.

To determine if Sema6D binds to endogenous Nr-CAM and Plexin-A1 on RGC axons, we applied AP-Sema6D to WT, *Nr-CAM*$^{-/-}$, *Plexin-A1*$^{-/-}$ or *Plexin-A1*$^{-/-}$*;Nr-CAM*$^{-/-}$ brain and optic chiasm sections. In both *Nr-CAM*$^{-/-}$ and *Plexin-A1*$^{-/-}$ chiasm, AP-Sema6D binding to RGC fibers in the chiasm was dramatically reduced compared to AP-Sema6D binding on WT chiasm sections, and binding to the *Plexin-A1*$^{-/-}$*;Nr-CAM*$^{-/-}$ chiasm was completely absent (Figure 6C).

To further characterize Nr-CAM interactions with Plexin-A1 and with Sema6D, we performed co-immunoprecipitation (IP) on HEK cells expressing Plexin-A1 and Nr-CAM, and on HEK cells expressing Nr-CAM and Sema6D. Vsv-tagged Plexin-A1 co-precipitated with Nr-CAM and v5-tagged Sema6D co-precipitated with Nr-CAM (Figures 6D and 6E). In contrast, vsv-tagged Plexin-A1 did not co-precipitate with Neurofascin. These results suggest that Nr-CAM can interact with both Sema6D and Plexin-A1.

We next determined whether Nr-CAM facilitates binding of Plexin-A1 to Sema6D. In a AP-Sema6D binding assay in HEK cells transfected with either Plexin-A1, Nr-CAM, or both, 1.3–2.3 times more HEK cells transfected with both Plexin-A1 and Nr-CAM displayed AP-Sema6D binding than cells transfected with Plexin-A1 only or Nr-CAM only (Figures S6B and S6C). We attempted to determine the binding affinity of AP-Sema6D to Plexin-A1 or Nr-CAM alone, and together, but AP-Sema6D binding to Plexin-A1 and Nr-CAM alone gave variable binding affinity values, possibly due to weak binding. Taken together, these data reveal several different Nr-CAM-Plexin-A1 binding scenarios: they could interact between or within RGC axons, between distinct chiasm cell populations, and/or between RGCs and chiasm cells to modify the inhibitory action of Sema6D.

Sema6D, Nr-CAM and Plexin-A1 at the optic chiasm midline are necessary for the formation of the crossed projection *in vivo*

To explore the role of Sema6D in chiasm formation in an intact brain, we added αSema6D to E14.5 WT brains in which the chiasm had been exposed. Brain preparations treated with αSema6D displayed a 37% increase in the size of the ipsilateral projection compared to brains treated with αcontrol (Figure S6) (embryos + αSema6D = 1.37±0.04 versus embryos + αCtr = 1.0±0.04, $p<0.01$). These results suggest that if Sema6D function is blocked, axons have a tendency to project ipsilaterally.

We next probed the role of Sema6D, Plexin-A1, and Nr-CAM in retinal axon decussation *in vivo* by examining the phenotype of the optic chiasm in *Sema6D*$^{-/-}$, *Nr-CAM*$^{-/-}$, *Plexin-A1*$^{-/-}$ and *Plexin-A1*$^{-/-}$;*Nr-CAM*$^{-/-}$ with anterograde DiI labeling (Figure 7A). At E14.5 and E15.5, the *Nr-CAM*$^{-/-}$ chiasm displayed no obvious defects in decussation (Williams et al., 2006). Further, the expression pattern of Neuropilin1, EphB1, Zic2, and Shh in Tuj1^{+} RGCs, and the expression of ephrin-B2, Shh, VEGF^{165} and Sema6D expression in the optic chiasm were similar in WT and *Plexin-A1*$^{-/-}$;*Nr-CAM*$^{-/-}$ mice (data not shown). The *Plexin-A1*$^{-/-}$ chiasm showed slight defasciculation of the contralateral projection at E14.5, but less so at E15.5. In contrast, in both the *Sema6D*$^{-/-}$ and *Plexin-A1*$^{-/-}$;*Nr-CAM*$^{-/-}$ chiasm at E14.5 the contralateral projection was more highly defasciculated compared to the contralateral projection chiasm of WT or *Plexin-A1*$^{-/-}$ embryos. In addition, the E15.5 *Sema6D*$^{-/-}$ and *Plexin-A1*$^{-/-}$;*Nr-CAM*$^{-/-}$ chiasm had a 68% and 87% larger ipsilateral projection, respectively, compared to the WT chiasm (WT = 1.0±0.04 versus *Sema6D*$^{-/-}$ = 1.68±0.01, $p<0.01$, *Nr-CAM*$^{-/-}$ = 1.03±0.01, $p>0.05$, *Plexin-A1*$^{-/-}$ = 0.96±0.01, $p>0.05$ and *Plexin-A1*$^{-/-}$;*Nr-CAM*$^{-/-}$ = 1.87±0.07, $p<0.01$) (Figure 7B). Moreover, in the *Sema6D*$^{-/-}$ and *Plexin-A1*$^{-/-}$;*Nr-CAM*$^{-/-}$ chiasm, many crossing fibers strayed from the chiasm caudally into the diencephalon, and some fibers looped back towards the ipsilateral optic tract (Figures 7A and 7B). At E18.5 and P0, *Plexin-A1*$^{-/-}$, *Sema6D*$^{-/-}$ and *Plexin-A1*$^{-/-}$;*Nr-CAM*$^{-/-}$ embryos still displayed a 28%, 60% and 53% larger ipsilateral projection, respectively, compared to WT (Figures S7A–C) (At E18.5, WT = 1.0±0.02 versus *Sema6D*$^{-/-}$ = 1.60±0.09, $p<0.01$. At P0, WT = 1.0±0.03 versus *Plexin-A1*$^{-/-}$ = 1.28±0.02, $p<0.01$ and *Plexin-A1*$^{-/-}$;*Nr-CAM*$^{-/-}$ = 1.53±0.04, $p<0.01$). Thus, in *Sema6D*$^{-/-}$ and *Nr-CAM*$^{-/-}$;*Plexin-A1*$^{-/-}$ mice, RGC axons defasciculate and project ipsilaterally more frequently than contralaterally.

An increased ipsilateral projection arises from non-VT retina in *Plexin-A1*$^{-/-}$;*Nr-CAM*$^{-/-}$ mice

Finally, we determined the retinotopic origin of fibers that aberrantly project ipsilaterally in WT and *Plexin-A1*$^{-/-}$;*Nr-CAM*$^{-/-}$ by retrograde labeling with DiI from the optic tract (Figure 8A). The number of DiI-labeled RGCs within the VT region was not increased compared to WT retina (WT = 84.9±10.1 versus *Plexin-A1*$^{-/-}$;*Nr-CAM*$^{-/-}$ = 85.5±8.4, $p>0.05$). However, in *Plexin-A1*$^{-/-}$;*Nr-CAM*$^{-/-}$ mice, DiI^{+} RGCs were ectopically located in non-VT regions of the ipsilateral retina (WT = 5.0±0.97 versus *Plexin-A1*$^{-/-}$;*Nr-CAM*$^{-/-}$ = 51.4±6.5, $p<0.01$) (Figure 8B). This result indicates that in the absence of Nr-CAM and Plexin-A1, non-VT RGCs that normally cross the midline are aberrantly routed into the ipsilateral optic tract.

Thus, in the absence of Sema6D or both Plexin-A1 and Nr-CAM *in vivo*, RGC axons defasciculate, misroute into the caudal diencephalon, and more frequently project into the ipsilateral optic tract.

Discussion

Cues responsible for the contralateral projection of retinal axons have long remained unclear. In this study we document a tripartite recognition system that actively regulates RGC midline crossing. Sema6D is the focal point of a molecular complex in which Plexin-A1 and Nr-CAM on chiasm cells engage Sema6D and switch the sign of Sema6D from growth-inhibiting to growth-promoting. This scheme provides a novel strategy for midline crossing: in particular, the modulation of ligand activity by accessory recognition proteins expressed by ligand-presenting cells. Such a guidance mechanism achieves a switch in ligand activity without changing expression of receptor subunits on responsive axons (Figures 8D and S8).

Switching the sign of Sema6D to direct RGC decussation at the optic chiasm

Our findings reveal that the interaction of Sema6D, Plexin-A1, and Nr-CAM on chiasm cells inverts the sign of Sema6D signaling and represents a switch mechanism crucial for chiasm crossing. The deployment of distinct receptor subunits has been shown to switch axonal responses to an individual guidance molecule in many different neural systems. As one example, Sema3E is a repulsive cue for distinct populations of forebrain axons that express Plexin-D1 alone, but when Neuropilin1 and Plexin-D1 are co-expressed by these axons, Sema3E signaling promotes rather than retards growth (Chauvet et al., 2007). In an analogous manner, the expression of the netrin receptor, unc5 and its vertebrate counterparts (UNC5H1-3) can change the response of its co-receptor unc40/DCC to the guidance factor unc-6/netrin from attraction to repulsion (Chisholm and Tessier-Lavigne, 1999; Culotti and Merz, 1998; Hong et al., 1999). In these and other instances, a change in the receptor complex expressed by axons underlies the switch in response to guidance cues. The scenario we describe in this study is conceptually different in that the expression of Nr-CAM and Plexin-A1 by ligand-presenting midline cells triggers the switch in axonal response.

Although we recognize the existence of other conceivable strategies for switching the response of RGCs to Sema6D (Figure S8), our data can best be explained by a model in which Nr-CAM and Plexin-A1 on chiasm cells modulate the interaction of the Sema6D ligand with Nr-CAM and Plexin-A1 receptors on RGCs. The fact that Plexin-A1 and Nr-CAM are expressed by the ligand presenting cells (midline glia and chiasm neurons) as well as by RGCs poses the question of how they change RGC axon interactions with Sema6D. One possibility is that Nr-CAM and Plexin-A1 on chiasm cells alter the conformation of the Nr-CAM and Plexin-A1 receptor system on RGCs. This altered receptor state would then transduce Sema6D signals in a manner different to that of Sema6D alone. An alternative idea is that the conformation of Sema6D on midline glia is changed by its interaction with Nr-CAM on midline glia and with Plexin-A1 on chiasm neurons, such that Sema6D association with the Nr-CAM/Plexin-A1 receptor system on RGC axons triggers growth rather than inhibition (Figure 8D). Evaluation *in vivo* of the phenotype of $Sema6D^{flox/flox}$, $Plexin\text{-}A1^{flox/flox}$ and $Nr\text{-}CAM^{flox/flox}$ mice will require the construction of new and more selective means of gene inactivation in chiasm cells. Furthermore, although the detailed organization of the Sema6D/Nr-CAM/Plexin-A1 receptor complex is not yet known, the structural characterization of semaphorin ligands bound to plexin receptors (Janssen et al., 2010; Nogi et al., 2010) could provide insights into such potential molecular interactions at the chiasm.

How the presentation of Nr-CAM, Plexin-A1 and Sema6D by the chiasm midline activates different downstream signaling cascades in RGCs compared to the action of Sema6D alone remains unclear. Downstream signaling cascades that switch attractive to repulsive responses have been described for Eph-ephrin interactions (Egea et al., 2005). The FAK/Src signaling pathway is activated in Sema3B-induced attraction, but not in Sema3B-induced repulsion (Falk et al., 2005). Similarly, a calmodulin-activated adenylate cyclase (ADCY8) is critical for antagonizing Slit-induced repulsion via the chemokine SDF1, and knockdown of ADCY8 restores sensitivity to slit and aberrantly drives RGC axons ipsilaterally (Xu et al., 2010).

RGC axon fasciculation at the optic chiasm

Fasciculation is critical for axon guidance (Raper and Mason, 2010). In the retina, disruptions in RGC fasciculation and coherence of the optic chiasm can occur independently of errors in midline crossing (Plump et al., 2002). In addition to their guidance function in switching Sema6D from growth inhibition to promotion, Nr-CAM, Plexin-A1 and Sema6D could regulate fasciculation of RGC axons as they cross the midline. The RGC projection is

defasciculated in *Sema6D*$^{-/-}$ and *Plexin-A1*$^{-/-}$*;Nr-CAM*$^{-/-}$ mice, more notably in axons that have already traversed the midline (Figure 7). In higher vertebrates, crossed axons from each eye rearrange into smaller bundles, interdigitating with each other as they traverse the midline (Colello and Guillery, 1998; Guillery et al., 1995). By modifying Sema6D inhibition, Nr-CAM-Plexin-A1 interactions at the midline could also function to split RGC axon fascicles axons into smaller units that facilitate penetration of radial glial fibers and extension across the midline. Insufficient defasciculation or fasciculation in the absence of Sema6D, Nr-CAM, and Plexin-A1 could impede axons from traversing the midline, leading to an increased ipsilateral projection, misrouting, and perturbed topographic connections in targets (Chan and Chung, 1999; Sakano, 2010).

Additional molecules for decussation at the optic chiasm?

Our data indicate that the growth supporting activity of the Sema6D, Nr-CAM, and Plexin-A1 complex at the optic chiasm is crucial for proper formation of the crossed pathway. However, in Sema6D $^{-/-}$ and *Plexin-A1*$^{-/-}$*;Nr-CAM*$^{-/-}$ mice, in which the chiasm is severely perturbed, the majority of non-VT axons still cross the midline. VEGF has been identified at the optic chiasm as a long-range cue that interacts with Neuropilin1 to attract crossing axons towards the midline (Erskine et al., 2011). *VEGF*$^{-/-}$ and *Nrp1*$^{-/-}$ mice display an increased ipsilateral projection. However, it is unclear if this phenotype results from disruption of an active crossing mechanism or from removal of an attractive midline cue that then results in passive redirecting of axons ectopically into the ipsilateral optic tract. Moreover, as with the mutant lines examined here, *VEGF*$^{-/-}$ and *Nrp1*$^{-/-}$ mice also retain a large contralateral projection. Thus, guidance cues other than VEGF and Sema6D may be involved in midline crossing and establishment of the crossed RGC axon pathway. Alternatively, the persistence of the contralateral projection in all of these mutants could reflect an underlying tendency of RGCs to cross the midline (Guillery et al., 1995). Crossing the midline may be an easier option than turning back into the ipsilateral optic tract. The tripartite system described here, as with VEGF/neuropilin signaling, could provide a necessary molecular “boost” that augments this inertial midline tendency.

Experimental Procedures

Mice

All animal procedures followed the regulatory guidelines of the Columbia University Institutional Animal Care and Use Committee. Noon of the day on which a plug was found was considered E0.5. Generation, breeding and genotyping of *Nr-CAM*$^{-/-}$, *Plexin-A1*$^{-/-}$ and *Sema6D*$^{-/-}$ mutants were described previously (Sakurai et al., 2001; Takamatsu et al., 2010; Yoshida et al., 2006). Mice were maintained on a 129SvEvS6 (*Nr-CAM*$^{-/-}$) or a C57BL/6 (*Plexin-A1*$^{-/-}$ and *Sema6D*$^{-/-}$) genetic background. *Plexin-A1*$^{-/-}$;*Nr-CAM*$^{-/-}$ double mutants were generated from these mutants resulting in a 129SvEvS6/C57BL/6 background. These mice are born at roughly Mendelian ratios, are fertile, and survive to adulthood.

DiI labeling

Whole anterograde and retrograde labeling was performed on fixed tissue using DiI (Molecular Probes) as described previously (Pak et al., 2004; Plump et al., 2002). For quantification of the ipsilateral projection in mutants anterogradely labeled with DiI, pixel intensity of DiI^{+} ipsilateral and contralateral optic tracts adjacent to chiasm midline in a 500 × 500 μm area measured with MetaMorph image analysis software. The ipsilateral index was obtained by dividing the intensity of the ipsilateral projection as seen in whole mounts by the sum of the contralateral and ipsilateral pixel intensities. Each of the ipsilateral indexes in mutants was normalized to the WT ipsilateral index. Details are shown in Figure7B.

Retina-chiasm cell cocultures

Retinal explants were dissected from E14.5 WT C57BL/6 or mutant embryos as described previously (Wang et al., 1996). To harvest chiasm cells, a 400 × 400 μm area of the ventral diencephalon that included the chiasm midline was dissected, dissociated and plated at a density of 140,000 cells/dish shortly after retinal explants were plated, in DMEM/F12 serum free medium containing 0.4% methylcellulose with 80μg/ml αSema6D or pre-immune serum added. Cultures were grown for 18 hrs and then fixed for 30 min with 4% PFA. Neurites were visualized with a monoclonal neurofilament antibody (2H3). The total area covered by neurites of individual explants was quantified by measuring pixel intensity with Openlab image analysis software. The amount of axon growth was normalized with respect to the outgrowth of DT or VT explants under control conditions, and indicated in the left-most bar in each graph. Each experiment was carried out at least three times, and within each experiment, at least four explants were treated in each experimental group. Explants with neurites emanating from only one region, or explants with few or no axons, independent of the condition, were excluded from quantitative analysis.

Retina – HEK cell cocultures

HEK cells were transfected with lipofectamine 2000 (Invitrogen) with combinations of vsv-Plexin-A1 (gift of A.W. Püschel, Westfalische Wilhelms-Universität Münster), v5-Sema6D and Nr-CAM. Two days later, cells were dissociated with trypsin/EDTA and plated at the density of 70,000 cells/dish after plating retinal explants. When HEK cells transfected with Nr-CAM and Sema6D were combined with HEK cells expressing Plexin-A1 or empty vector, cells were mixed 1:1 and plated at 70,000 cells/dish. Neurite outgrowth was analyzed as described above.

Cultured intact visual system

E14.5 heads were dissected and the skin and upper palate removed to expose the optic chiasm. These exposed brain preparations were described previously (Williams et al., 2003). To block Sema6D, 80μg/ml of Sema6D antibody or pre-immune serum was added to the medium. Cultures were fixed with 4% PFA overnight. DiI was placed in one retina and labeled for 5 days at room temperature. Fluorescent images were taken with an Axiocam digital camera on an Axioplan 2 upright or Stemi SV11 dissecting Zeiss microscope. The size of the ipsilateral projection in exposed brain preparations treated with Sema6D or control antibody was quantified by the method described above for anterograde DiI labeling.

In situ hybridization and Immunohistochemistry

In situ hybridization using DIG-labeled probes for Plexin-A1, -A2, -A4, Neuropilin-1, Sema6A, -6B, -6C, -3A, -3B, -3D (Invitrogen), Shh (gift of P. Bovolenta, Universidad Autónoma de Madrid), VEGF165 (gift of C. Ruhrberg, University College, London), EphB1, ephrin-B2, Sema6D and Nr-CAM were performed as described previously (Williams et al., 2006; Williams et al., 2003; Yoshida et al., 2006). Immunolabeling of retinal explant cultures, retina-chiasm cocultures, and cryosections was performed with the following primary antibodies: mouse IgG anti-neurofilament (2H3, 1:5), mouse IgM anti-TAG-1 (4D7, 1:100), rabbit anti-Neurofascin (1:2000), rabbit anti-Nr-CAM837 (1:500), mouse IgG anti-L1CAM (2C2, 1:500; Abcam), goat IgG anti-Neuropilin1 (1:500; R&D systems), rabbit anti-Zic2 (1:10000; gift of S. Brown, Columbia University), mouse IgM anti-RC2 (1:4), mouse IgG bIII-tubulin (Tuj1) (1:1000; Sigma), mouse IgM anti-SSEA-1 (1:5), rabbit anti-Sema6D (1:400), and rabbit anti-Plexin-A1 (1:500) antibodies. Cy3, Cy5 (Jackson) or AlexFluor488 (Molecular Probes) were used as secondary antibodies. Hoechst 33258 (Molecular Probes) was used for nuclear staining. Images were captured with an Axiocam digital camera on a Zeiss Axioplan 2 microscope.

Binding assays

For co-immunoprecipitation assays, HEK293 cells were transfected with cDNAs encoding full-length Nr-CAM and vsv-tagged Plexin-A1 or v5-tagged Sema6D. Co-immunoprecipitation assays were performed as described (Castellani et al., 2000). Immunoprecipitated proteins were detected by anti-Nr-CAM (1:500), anti-v5 (1:1000; Invitrogen) and anti-vsv (1:500;Sigma). An alkaline phosphatase binding assay was performed as described previously (Yoshida et al., 2006). AP-Sema6D-Fc, AP-Sema6A or AP-Sema6C (gift of H. Fujisawa, Nagoya University) were transfected into HEK293 cells and the protein was purified from culture supernatants. To assess binding, HEK293 cells were transiently transfected with expression vectors encoding Plexin-A1 (gift of AW. Püschel), Neuropilin-1 (gift of R.J. Giger, University of Michigan), Nr-CAM, L1 (gift of D. Felsenfeld, Mount Sinai School of Medicine), TAG-1 (gift of A. Furley, University of Sheffield), or Neurofascin 186 (gift of V. Bennett, Duke University). AP-fusion protein binding to tissue sections were performed as described previously (Yoshida et al., 2006).

Statistical tests

All data were analyzed, and graphs were constructed using OpenLab imaging software Metamorph software or Microsoft Excel. All error bars represent the standard error of the mean (SEM), and statistical analysis was determined using one-way ANOVA followed by the Tukey's post hoc test, where appropriate. *$p<0.01$, N.S. Not significant ($p>0.05$).

Highlights

Plexin-A1 and Nr-CAM is expressed in contralateral RGCs and the optic chiasm midline.

Nr-CAM and Plexin-A1 modulate inhibition by midline Sema6D.

Nr-CAM is a novel receptor for Sema6D and binds to Plexin-A1.

Proper RGC axon fasciculation and decussation are dependent on all three factors.

Supplementary Material

Refer to Web version on PubMed Central for supplementary material.

Acknowledgments

We thank members of the Mason lab, Jane Dodd, Jon Terman and Alex Kolodkin for helpful comments on the experiments and manuscript. This work was supported by National Institutes of Health grants EY12736 (C.M.) and NS065048 (Y.Y.), the Howard Hughes Medical Institute (T.M.J.), Uehara Foundation (T.K.), Ministry of Health, Labour and Welfare, Program for Promotion of Fundamental Studies in Health Sciences of the National Institute of Biomedical Innovation, and Target Protein Research Program of the Japan Science and Technology Agency (A.K.), and Ministry of Education, Culture, Sports, Science and Technology of Japan, and the Japan Society for the Promotion of Science (N.T.)

REFERENCES

Bechara A, Falk J, Moret F, Castellani V. Modulation of semaphorin signaling by Ig superfamily cell adhesion molecules. Adv Exp Med Biol. 2007; 600:61–72. [PubMed: 17607947]

Castellani V, Chedotal A, Schachner M, Faivre-Sarrailh C, Rougon G. Analysis of the L1-deficient mouse phenotype reveals cross-talk between Sema3A and L1 signaling pathways in axonal guidance. Neuron. 2000; 27:237–249. [PubMed: 10985345]

Castellani V, De Angelis E, Kenwrick S, Rougon G. Cis and trans interactions of L1 with neuropilin-1 control axonal responses to semaphorin 3A. EMBO J. 2002; 21:6348–6357. [PubMed: 12456642]

Chan SO, Chung KY. Changes in axon arrangement in the retinofugal [correction of retinofungal] pathway of mouse embryos: confocal microscopy study using single- and double-dye label. J Comp Neurol. 1999; 406:251–262. [PubMed: 10096609]

Chauvet S, Cohen S, Yoshida Y, Fekrane L, Livet J, Gayet O, Segu L, Buhot MC, Jessell TM, Henderson CE, et al. Gating of Sema3E/PlexinD1 signaling by neuropilin-1 switches axonal repulsion to attraction during brain development. Neuron. 2007; 56:807–822. [PubMed: 18054858]

Chisholm A, Tessier-Lavigne M. Conservation and divergence of axon guidance mechanisms. Curr Opin Neurobiol. 1999; 9:603–615. [PubMed: 10508749]

Colello SJ, Guillery RW. The changing pattern of fibre bundles that pass through the optic chiasm of mice. Eur J Neurosci. 1998; 10:3653–3663. [PubMed: 9875344]

Culotti JG, Merz DC. DCC and netrins. Curr Opin Cell Biol. 1998; 10:609–613. [PubMed: 9818171]

Derijck AA, Van Erp S, Pasterkamp RJ. Semaphorin signaling: molecular switches at the midline. Trends Cell Biol. 2010; 20:568–576. [PubMed: 20655749]

Dickson BJ, Zou Y. Navigating intermediate targets: the nervous system midline. Cold Spring Harb Perspect Biol. 2010; 2 a002055.

Egea J, Nissen UV, Dufour A, Sahin M, Greer P, Kullander K, Mrsic-Flogel TD, Greenberg ME, Kiehn O, Vanderhaeghen P, et al. Regulation of EphA 4 kinase activity is required for a subset of axon guidance decisions suggesting a key role for receptor clustering in Eph function. Neuron. 2005; 47:515–528. [PubMed: 16102535]

Erskine L, Herrera E. The retinal ganglion cell axon's journey: insights into molecular mechanisms of axon guidance. Dev Biol. 2007; 308:1–14. [PubMed: 17560562]

Erskine L, Reijntjes S, Pratt T, Denti L, Schwarz Q, Vieira JM, Alakakone B, Shewan D, Ruhrberg C. VEGF Signaling through Neuropilin 1 Guides Commissural Axon Crossing at the Optic Chiasm. Neuron. 2011; 70:951–965. [PubMed: 21658587]

Falk J, Bechara A, Fiore R, Nawabi H, Zhou H, Hoyo-Becerra C, Bozon M, Rougon G, Grumet M, Puschel AW, et al. Dual functional activity of semaphorin 3B is required for positioning the anterior commissure. Neuron. 2005; 48:63–75. [PubMed: 16202709]

Garcia-Frigola C, Carreres MI, Vegar C, Mason C, Herrera E. Zic2 promotes axonal divergence at the optic chiasm midline by EphB1-dependent and -independent mechanisms. Development. 2008; 135:1833–1841. [PubMed: 18417618]

Guillery RW, Mason CA, Taylor JS. Developmental determinants at the mammalian optic chiasm. J Neurosci. 1995; 15:4727–4737. [PubMed: 7623106]

Herrera E, Brown L, Aruga J, Rachel RA, Dolen G, Mikoshiba K, Brown S, Mason CA. Zic2 patterns binocular vision by specifying the uncrossed retinal projection. Cell. 2003; 114:545–557. [PubMed: 13678579]

Hong K, Hinck L, Nishiyama M, Poo MM, Tessier-Lavigne M, Stein E. A ligand-gated association between cytoplasmic domains of UNC5 and DCC family receptors converts netrin-induced growth cone attraction to repulsion. Cell. 1999; 97:927–941. [PubMed: 10399920]

Hornberger MR, Dutting D, Ciossek T, Yamada T, Handwerker C, Lang S, Weth F, Huf J, Wessel R, Logan C, et al. Modulation of EphA receptor function by coexpressed ephrinA ligands on retinal ganglion cell axons. Neuron. 1999; 22:731–742. [PubMed: 10230793]

Janssen BJ, Robinson RA, Perez-Branguli F, Bell CH, Mitchell KJ, Siebold C, Jones EY. Structural basis of semaphorin-plexin signalling. Nature. 2010; 467:1118–1122. [PubMed: 20877282]

Lee R, Petros TJ, Mason CA. Zic2 regulates retinal ganglion cell axon avoidance of ephrinB2 through inducing expression of the guidance receptor EphB1. J Neurosci. 2008; 28:5910–5919. [PubMed: 18524895]

Lustig M, Erskine L, Mason CA, Grumet M, Sakurai T. Nr-CAM expression in the developing mouse nervous system: ventral midline structures, specific fiber tracts, and neuropilar regions. J Comp Neurol. 2001; 434:13–28. [PubMed: 11329126]

Maness PF, Schachner M. Neural recognition molecules of the immunoglobulin superfamily: signaling transducers of axon guidance and neuronal migration. Nat Neurosci. 2007; 10:19–26. [PubMed: 17189949]

Mann F, Ray S, Harris W, Holt C. Topographic mapping in dorsoventral axis of the Xenopus retinotectal system depends on signaling through ephrin-B ligands. Neuron. 2002; 35:461–473. [PubMed: 12165469]

Marquardt T, Shirasaki R, Ghosh S, Andrews SE, Carter N, Hunter T, Pfaff SL. Coexpressed EphA receptors and ephrin-A ligands mediate opposing actions on growth cone navigation from distinct membrane domains. Cell. 2005; 121:127–139. [PubMed: 15820684]

Mason CA, Sretavan DW. Glia, neurons, and axon pathfinding during optic chiasm development. Curr Opin Neurobiol. 1997; 7:647–653. [PubMed: 9384544]

Moret F, Renaudot C, Bozon M, Castellani V. Semaphorin and neuropilin coexpression in motoneurons sets axon sensitivity to environmental semaphorin sources during motor axon pathfinding. Development. 2007; 134:4491–4501. [PubMed: 18039974]

Nakagawa S, Brennan C, Johnson KG, Shewan D, Harris WA, Holt CE. Ephrin-B regulates the Ipsilateral routing of retinal axons at the optic chiasm. Neuron. 2000; 25:599–610. [PubMed: 10774728]

Nawabi H, Briancon-Marjollet A, Clark C, Sanyas I, Takamatsu H, Okuno T, Kumanogoh A, Bozon M, Takeshima K, Yoshida Y, et al. A midline switch of receptor processing regulates commissural axon guidance in vertebrates. Genes Dev. 2010; 24:396–410. [PubMed: 20159958]

Niquille M, Garel S, Mann F, Hornung JP, Otsmane B, Chevalley S, Parras C, Guillemot F, Gaspar P, Yanagawa Y, et al. Transient neuronal populations are required to guide callosal axons: a role for semaphorin 3C. PLoS Biol. 2009; 7 e1000230.

Nogi T, Yasui N, Mihara E, Matsunaga Y, Noda M, Yamashita N, Toyofuku T, Uchiyama S, Goshima Y, Kumanogoh A, et al. Structural basis for semaphorin signalling through the plexin receptor. Nature. 2010; 467:1123–1127. [PubMed: 20881961]

Pak W, Hindges R, Lim YS, Pfaff SL, O'Leary DD. Magnitude of binocular vision controlled by islet-2 repression of a genetic program that specifies laterality of retinal axon pathfinding. Cell. 2004; 119:567–578. [PubMed: 15537545]

Pecho-Vrieseling E, Sigrist M, Yoshida Y, Jessell TM, Arber S. Specificity of sensory-motor connections encoded by Sema3e-Plxnd1 recognition. Nature. 2009; 459:842–846. [PubMed: 19421194]

Petros TJ, Bryson JB, Mason C. Ephrin-B2 elicits differential growth cone collapse and axon retraction in retinal ganglion cells from distinct retinal regions. Dev Neurobiol. 2010

Petros TJ, Rebsam A, Mason CA. Retinal axon growth at the optic chiasm: to cross or not to cross. Annu Rev Neurosci. 2008; 31:295–315. [PubMed: 18558857]

Petros TJ, Shrestha BR, Mason C. Specificity and sufficiency of EphB1 in driving the ipsilateral retinal projection. J Neurosci. 2009; 29:3463–3474. [PubMed: 19295152]

Petros TJ, Williams SE, Mason CA. Temporal regulation of EphA4 in astroglia during murine retinal and optic nerve development. Mol Cell Neurosci. 2006; 32:49–66. [PubMed: 16574431]

Piper M, Plachez C, Zalucki O, Fothergill T, Goudreau G, Erzurumlu R, Gu C, Richards LJ. Neuropilin 1-Sema signaling regulates crossing of cingulate pioneering axons during development of the corpus callosum. Cereb Cortex. 2009; 19(Suppl 1):i11–i21. [PubMed: 19357391]

Plump AS, Erskine L, Sabatier C, Brose K, Epstein CJ, Goodman CS, Mason CA, Tessier-Lavigne M. Slit1 and Slit2 cooperate to prevent premature midline crossing of retinal axons in the mouse visual system. Neuron. 2002; 33:219–232. [PubMed: 11804570]

Raper J, Mason C. Cellular strategies of axonal pathfinding. Cold Spring Harb Perspect Biol. 2010; 2 a001933.

Runker AE, Little GE, Suto F, Fujisawa H, Mitchell KJ. Semaphorin-6A controls guidance of corticospinal tract axons at multiple choice points. Neural Dev. 2008; 3:34. [PubMed: 19063725]

Sakai JA, Halloran MC. Semaphorin 3d guides laterality of retinal ganglion cell projections in zebrafish. Development. 2006; 133:1035–1044. [PubMed: 16467361]

Sakano H. Neural map formation in the mouse olfactory system. Neuron. 2010; 67:530–542. [PubMed: 20797531]

Sakurai T, Lustig M, Babiarz J, Furley AJ, Tait S, Brophy PJ, Brown SA, Brown LY, Mason CA, Grumet M. Overlapping functions of the cell adhesion molecules Nr-CAM and L1 in cerebellar granule cell development. J Cell Biol. 2001; 154:1259–1273. [PubMed: 11564762]

Suto F, Ito K, Uemura M, Shimizu M, Shinkawa Y, Sanbo M, Shinoda T, Tsuboi M, Takashima S, Yagi T, et al. Plexin-a4 mediates axon-repulsive activities of both secreted and transmembrane semaphorins and plays roles in nerve fiber guidance. J Neurosci. 2005; 25:3628–3637. [PubMed: 15814794]

Takamatsu H, Takegahara N, Nakagawa Y, Tomura M, Taniguchi M, Friedel RH, Rayburn H, Tessier-Lavigne M, Yoshida Y, Okuno T, et al. Semaphorins guide the entry of dendritic cells into the lymphatics by activating myosin II. Nat Immunol. 2010

Takegahara N, Takamatsu H, Toyofuku T, Tsujimura T, Okuno T, Yukawa K, Mizui M, Yamamoto M, Prasad DV, Suzuki K, et al. Plexin-A1 and its interaction with DAP12 in immune responses and bone homeostasis. Nat Cell Biol. 2006; 8:615–622. [PubMed: 16715077]

Toyofuku T, Zhang H, Kumanogoh A, Takegahara N, Suto F, Kamei J, Aoki K, Yabuki M, Hori M, Fujisawa H, et al. Dual roles of Sema6D in cardiac morphogenesis through region-specific association of its receptor, Plexin-A1, with off-track and vascular endothelial growth factor receptor type 2. Genes Dev. 2004; 18:435–447. [PubMed: 14977921]

Wang LC, Dani J, Godement P, Marcus RC, Mason CA. Crossed and uncrossed retinal axons respond differently to cells of the optic chiasm midline in vitro. Neuron. 1995; 15:1349–1364. [PubMed: 8845158]

Wang LC, Rachel RA, Marcus RC, Mason CA. Chemosuppression of retinal axon growth by the mouse optic chiasm. Neuron. 1996; 17:849–862. [PubMed: 8938118]

Williams SE, Grumet M, Colman DR, Henkemeyer M, Mason CA, Sakurai T. A role for Nr-CAM in the patterning of binocular visual pathways. Neuron. 2006; 50:535–547. [PubMed: 16701205]

Williams SE, Mann F, Erskine L, Sakurai T, Wei S, Rossi DJ, Gale NW, Holt CE, Mason CA, Henkemeyer M. Ephrin-B2 and EphB1 mediate retinal axon divergence at the optic chiasm. Neuron. 2003; 39:919–935. [PubMed: 12971893]

Wolman MA, Regnery AM, Becker T, Becker CG, Halloran MC. Semaphorin3D regulates axon axon interactions by modulating levels of L1 cell adhesion molecule. J Neurosci. 2007; 27:9653–9663. [PubMed: 17804626]

Xu H, Leinwand SG, Dell AL, Fried-Cassorla E, Raper JA. The calmodulin-stimulated adenylate cyclase ADCY8 sets the sensitivity of zebrafish retinal axons to midline repellents and is required for normal midline crossing. J Neurosci. 2010; 30:7423–7433. [PubMed: 20505109]

Yates PA, Holub AD, McLaughlin T, Sejnowski TJ, O'Leary DD. Computational modeling of retinotopic map development to define contributions of EphA-ephrinA gradients, axon-axon interactions, and patterned activity. J Neurobiol. 2004; 59:95–113. [PubMed: 15007830]

Yoshida Y, Han B, Mendelsohn M, Jessell TM. PlexinA1 signaling directs the segregation of proprioceptive sensory axons in the developing spinal cord. Neuron. 2006; 52:775–788. [PubMed: 17145500]

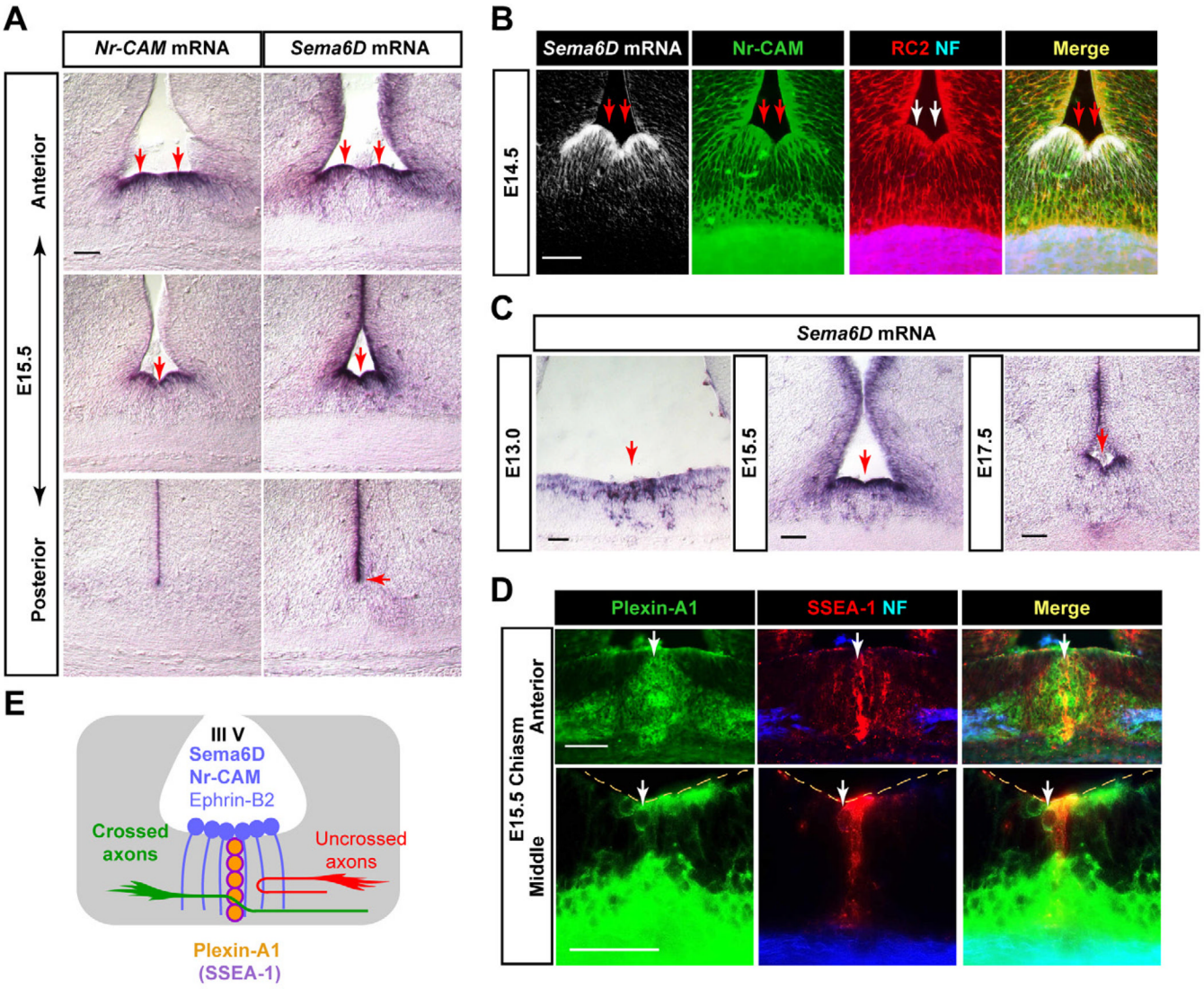

Figure 1. Expression of Sema6D and Plexin-A1 at the optic chiasm

(A) Sema6D and Nr-CAM are expressed in radial glia at the chiasm midline at E15.5, but Sema6D extends further dorsally in the VZ. (B) Sema6D mRNA is expressed in Nr-CAM$^+$ (green)/RC2$^+$ (red) radial glia at E14.5. Retinal axons stained with neurofilament antibody (NF, blue) extend through radial glial processes. (C) Sema6D mRNA is expressed in radial glial cell bodies at the floor of the third ventricle in the optic chiasm and along the ventricular zone at E13.0, E15.5 and E17.5. (D) Plexin-A1 expression at the E15.5 optic chiasm in cells in the ventral diencephalon. In frontal sections, Plexin-A1 protein (green) is colocalized with SSEA-1 (red) in chiasmatic neurons at the midline raphe and also on neurofilament$^+$ retinal axons (blue). (E) Schema of Sema6D and Plexin-A1 expression at the optic chiasm, depicted in frontal planes. Note that Sema6D is expressed by Nr-CAM$^+$/ephrin-B2$^+$ radial glial cells, and Plexin-A1 is expressed by SSEA-1$^+$ chiasm neurons. Scale bars: 100μm.

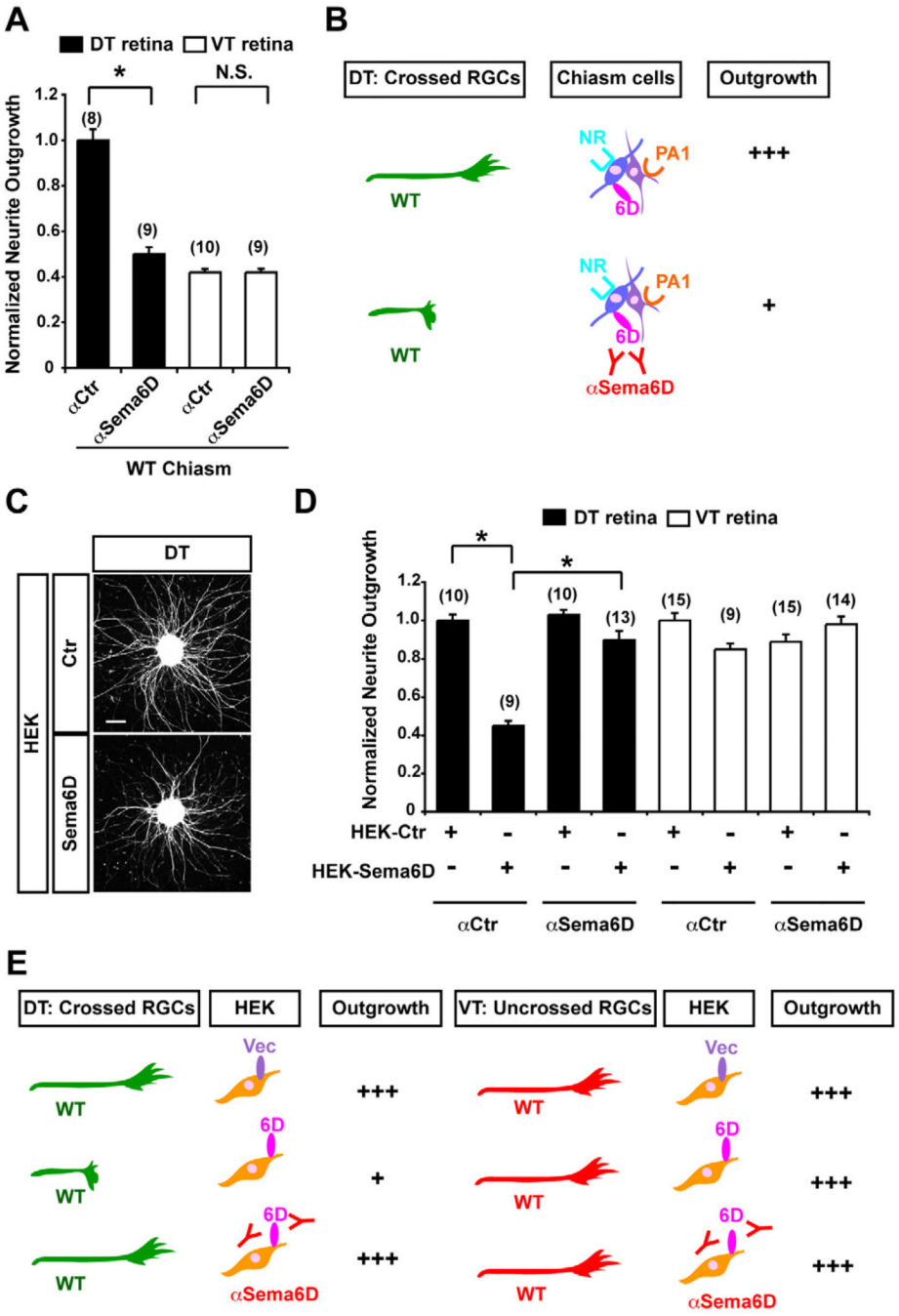

Figure 2. Sema6D is inhibitory to outgrowth of crossed RGCs *in vitro*

(A) A Sema6D function–blocking antibody (αSema6D) specifically reduces RGC neurite outgrowth from DT explants, but has no effect on VT explants on WT chiasm cells. (B) Summary of results in Figure 2A. Note that blocking Sema6D functions leads to less supportive to outgrowth of crossed RGC axons. (C) Representative E14.5 DT explants plated on HEK cells expressing an empty vector (Ctr) or Sema6D. (D) DT neurite outgrowth is reduced on Sema6D^{+} HEK cells, but this growth reduction is not observed in the presence of αSema6D. VT outgrowth is not changed from control levels in explants growth on Sema6D^{+} HEK cells, with or without αSema6D. (E) Summary of results in Figure 2D. Note

that Sema6D^{+} HEK cells are inhibitory to neurite outgrowth from crossed RGC axons. Scale bars: 200μm, (n) = number of explants for each condition, * $p<0.01$.

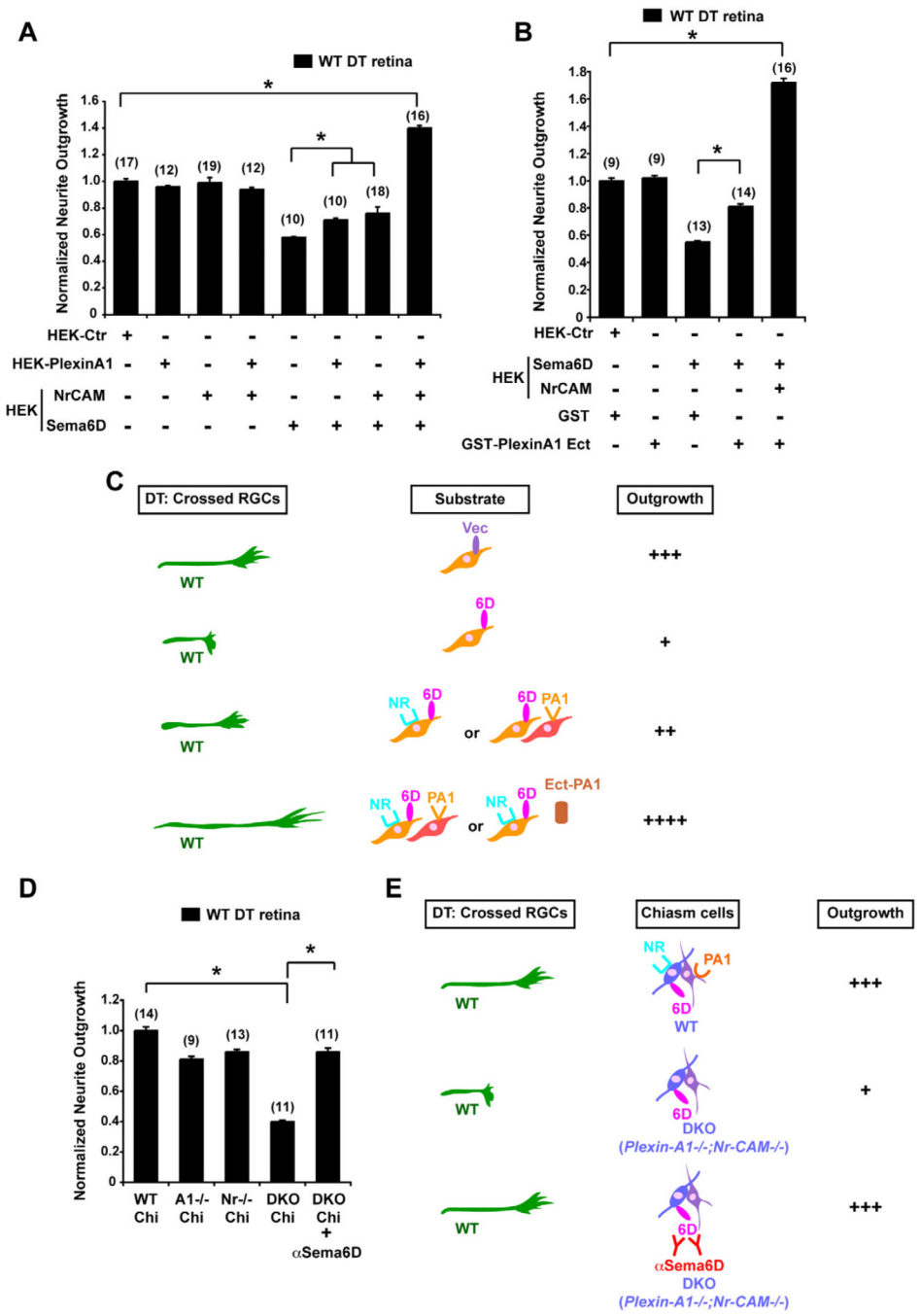

Figure 3. Nr-CAM and Plexin-A1 in cells of the optic chiasm convert the inhibitory effect of Sema6D on crossed RGCs to growth-promotion

(A) Quantification of WT DT retinal outgrowth on Sema6D$^+$/Nr-CAM$^+$ HEK cells and/or Plexin-A1$^+$ HEK cells. Note that inhibition of DT outgrowth by Sema6D is partially alleviated by Plexin-A1$^+$ or by Nr-CAM$^+$ HEK cells. However, DT neurite outgrowth is greatly enhanced (by ~40%) in the presence of Sema6D$^+$/Nr-CAM$^+$ HEK cells cocultured with Plexin-A1$^+$ HEK cells. (B) Quantification of WT DT retinal outgrowth on Sema6D$^+$/Nr-CAM$^+$ HEK cells in the presence of 100μg/ml GST-Plexin-A1 ectodomain or GST proteins. DT RGC outgrowth is poor on Sema6D$^+$ HEK cells, but inhibition is partially alleviated by the addition of GST-Plexin-A1. However, DT neurite outgrowth on Sema6D$^+$/

Nr-CAM^{+} HEK cells is greatly enhanced (by ~70%) in the presence of GST-Plexin-A1. (n) = number of explants for each condition, * $p<0.01$ (C) Summary of results in Figures 3A and B. Note that outgrowth of crossed RGC axons is enhanced on Sema6D^{+}/Nr-CAM^{+} HEK cells cocultured with Plexin-A1^{+} HEK cells and especially by GST-Plexin-A1 ectodomain. (D) Quantification of WT DT retinal outgrowth on *Plexin-A1*$^{-/-}$ (A1$^{-/-}$), *Nr-CAM*$^{-/-}$ (Nr$^{-/-}$) single mutant or *Plexin-A1*$^{-/-}$*;Nr-CAM*$^{-/-}$ (DKO) double mutant chiasm cells. (E) Summary of results in Figure 3D. Note that DKO chiasm cells are unsupportive of WT RGC neurite outgrowth, but with αSema6D DT neurite outgrowth is partially restored. (n) = number of explants for each condition, * $p<0.01$

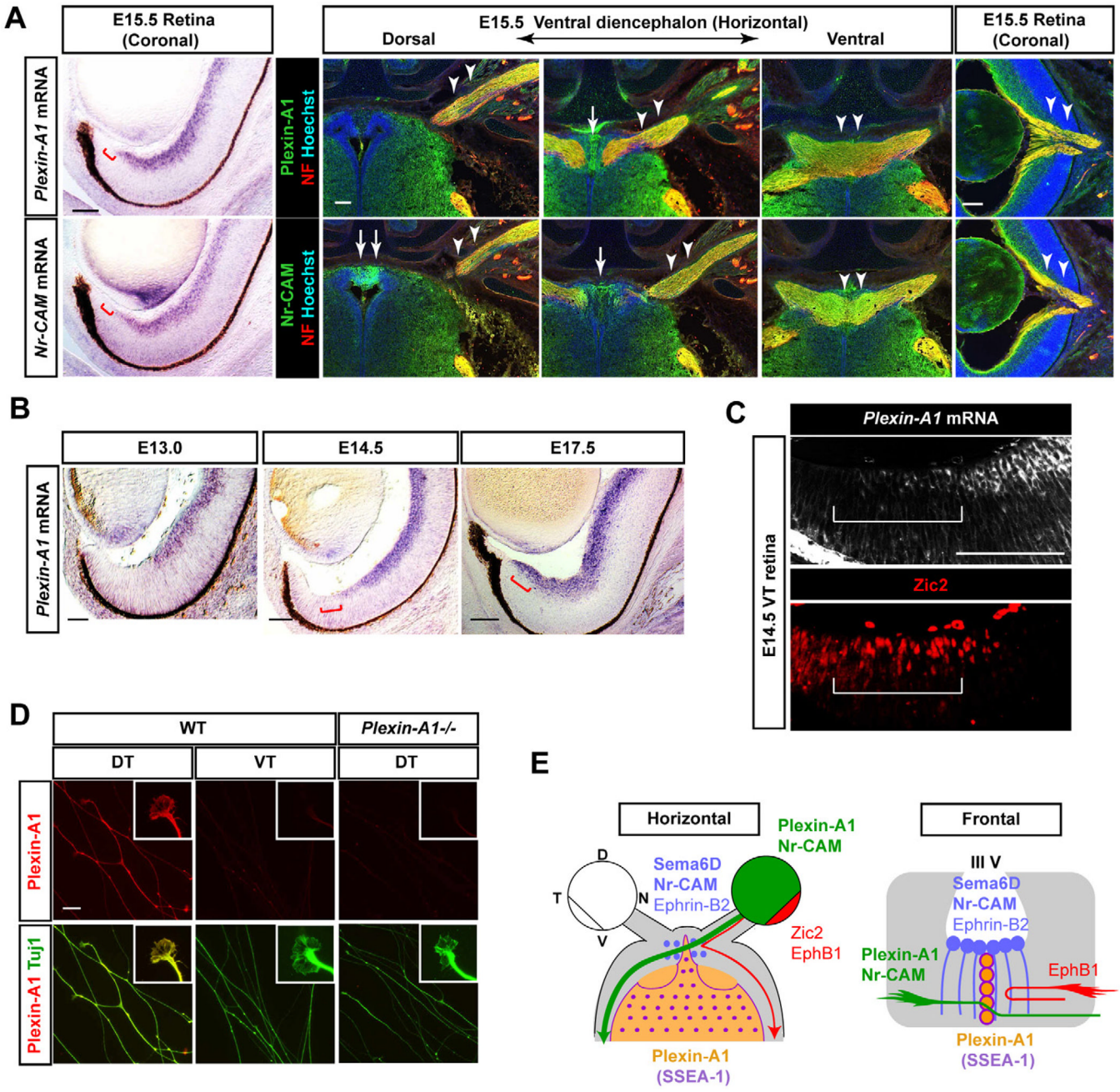

Figure 4. Expression of Plexin-A1, a receptor for Sema6D in crossed RGCs

(A) At E15.5 Plexin-A1 and Nr-CAM mRNA (left panels) and proteins (right panels) are similarly expressed in RGCs outside of the VT crescent (red bars) and retinal axons (arrowheads), but they are distinctly expressed in chiasm regions (arrows) in serial sections. (B) Plexin-A1 mRNA is expressed in the central retina at E13.0, in RGCs outside of the VT crescent at E14.5 and in these RGCs and those in the VT retina at E17.5 (red bars). (C) Plexin-A1 is not expressed by $Zic2^{+}$ RGCs in E14.5 VT (white bar). (D) Plexin-A1 is expressed on DT (crossed) axons and growth cones but not VT (uncrossed) or *Plexin-A1*$^{-/-}$ DT axons. (E) Schema of Plexin-A1 expression in crossed axons and in the chiasm area. Scale bars: 100μm in A–C; 20μm in D.

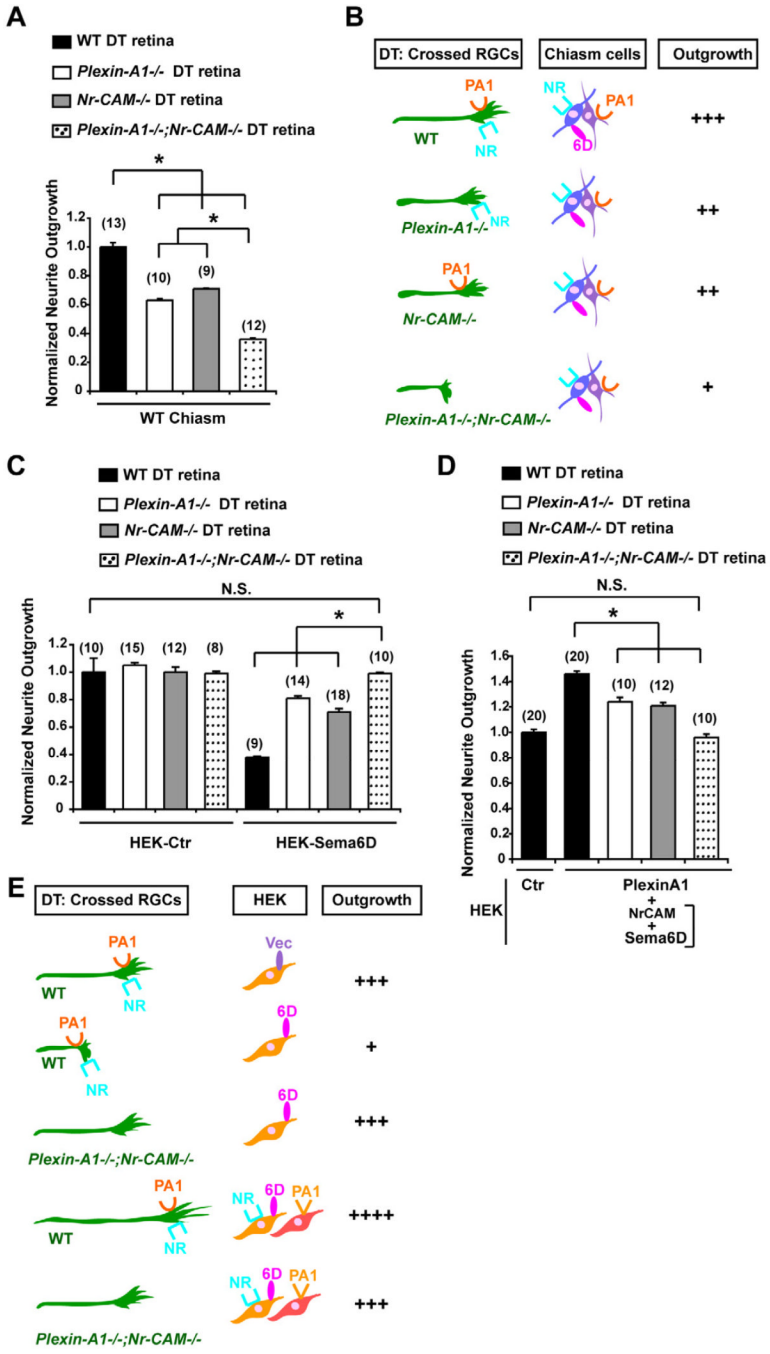

Figure 5. Nr-CAM and Plexin-A1 in crossed RGCs mediate effects of Sema6D on RGC outgrowth

(A) Outgrowth of *Plexin-A1*$^{-/-}$*;Nr-CAM*$^{-/-}$ DT explants is reduced on WT chiasm cells compared to WT, *Plexin-A1*$^{-/-}$ single or *Nr-CAM*$^{-/-}$ DT explants. (B) Summary of results in Figure 5A. Note that outgrowth of *Plexin-A1*$^{-/-}$ or *Nr-CAM*$^{-/-}$ DT explants are only partially reduced, but outgrowth of *Plexin-A1*$^{-/-}$*;Nr-CAM*$^{-/-}$ DT explants are further reduced on WT chiasm cells. (C) Quantification of *Nr-CAM*$^{-/-}$, *Plexin-A1*$^{-/-}$ and *Plexin-A1*$^{-/-}$*;Nr-CAM*$^{-/-}$ outgrowth from DT retinal explants on Sema6D^{+} HEK cells. Note that Sema6D^{+} HEK cells only partially inhibit outgrowth of *Nr-CAM*$^{-/-}$ or *Plexin-A1*$^{-/-}$ DT explants, but neurite outgrowth is similar to controls in *Plexin-A1*$^{-/-}$*;Nr-CAM*$^{-/-}$ DT

explants. (D) Outgrowth of *Nr-CAM*$^{-/-}$, *Plexin-A1*$^{-/-}$ and *Plexin-A1*$^{-/-}$*;Nr-CAM*$^{-/-}$ DT retinal outgrowth on Sema6D^{+}/Nr-CAM^{+} and Plexin-A1^{+} HEK cells. (E) Summary of results in Figures 5C and 5D. Note that *Plexin-A1*$^{-/-}$*;Nr-CAM*$^{-/-}$ DT axons grew no differently on Sema6D^{+} HEK cells or on Sema6D^{+}/Nr-CAM^{+} and Plexin-A1^{+} HEK cells than on HEK cells expressing empty vector. (n) = number of explants for each condition, * $p<0.01$

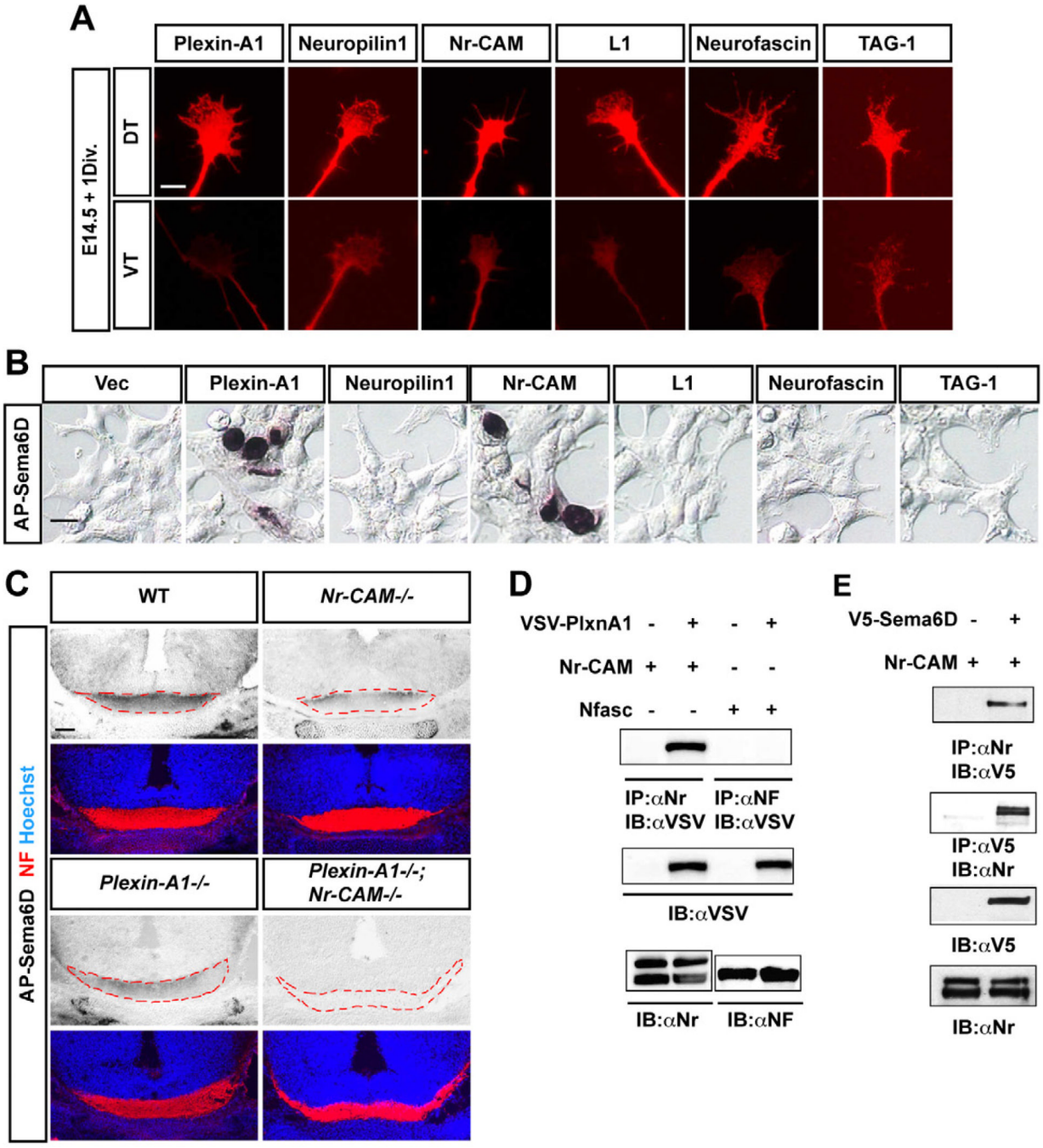

Figure 6. Nr-CAM is a receptor for Sema6D

(A) Expression of Plexin-A1, Neuropilin1, Nr-CAM, Neurofascin, TAG-1 and L1 are more highly expressed on DT axons and growth cones compared to VT. (B) AP-Sema6D binds to HEK cells transfected with Plexin-A1 or Nr-CAM, but not Neuropilin1 and other CAMs. (C) AP-Sema6D binding to retinal axons (red, neurofilament (NF)) is reduced in *Nr-CAM*$^{-/-}$ and *Plexin-A1*$^{-/-}$ mutant brain sections through the optic chiasm compared to WT and is completely absent in *Plexin-A1*$^{-/-}$*;Nr-CAM*$^{-/-}$ double mutant brains. (D) Immunoprecipitation assay demonstrating binding of Nr-CAM, but not Neurofascin 186 (Nfasc) to Plexin-A1. (E) Immunoprecipitation assay showing Nr-CAM and Sema6D binding. Scale bars, 5μm in A; 20μm in B; 200μm in C.

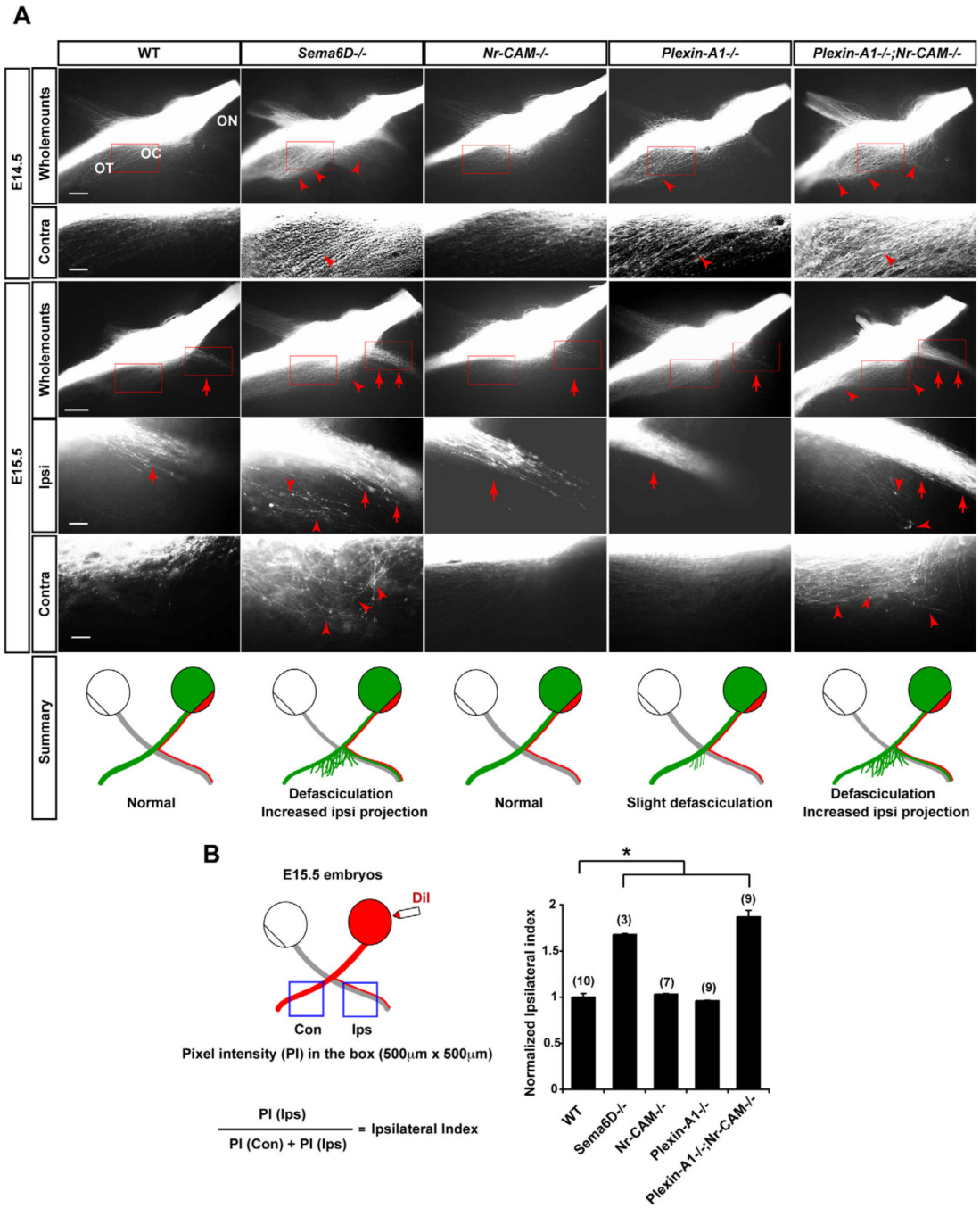

Figure 7. Sema6D, Nr-CAM and Plexin-A1 are important for formation of the crossed RGC projection *in vivo*

(A) Whole mounts of the optic chiasm in E14.5 and E15.5 WT, *Sema6D*$^{-/-}$, *Nr-CAM*$^{-/-}$, *Plexin-A1*$^{-/-}$ or *Plexin-A1*$^{-/-}$*;Nr-CAM*$^{-/-}$ mutants unilaterally labeled with DiI in the retina at the optic disc. E14.5 and E15.5 both *Nr-CAM*$^{-/-}$ and *Plexin-A1*$^{-/-}$ mutant chiasm have a normal ipsilateral projection (arrows) and only slight defasciculation of the contralateral projection (arrowhead) at E14.5. In contrast, in E14.5 *Sema6D*$^{-/-}$ and *Plexin-A1*$^{-/-}$*;Nr-CAM*$^{-/-}$ mutant chiasms, RGC axons on the side of the chiasm contralateral to the midline are defasciculated (arrowheads); at E15.5 both ipsi- and contralateral projections in these mutants are highly defasciculated (arrowheads) and the ipsilateral projection is greatly

increased (arrows). (n ≥ 3 embryos for each condition). Schematic depicts a summary of WT and mutant chiasm phenotypes. (B) Quantification of decussation defects in E15.5 *Sema6D*$^{-/-}$ single and *Plexin-A1*$^{-/-}$*;Nr-CAM*$^{-/-}$ double mutant embryos. Schematic presentation shows the measurement of pixel intensities of contralateral and ipsilateral optic tracts and the calculation to obtain an ipsilateral index. *Sema6D*$^{-/-}$ and *Plexin-A1*$^{-/-}$*;Nr-CAM*$^{-/-}$ mutants display a 1.6–1.9 times larger ipsilateral projection compared to WT, *Nr-CAM*$^{-/-}$ and *Plexin-A1*$^{-/-}$ chiasm. ON, optic nerve; OT, optic tract; OC, optic chiasm. Scale bars, 200μm in low-magnification images; 20μm in high-magnification images, (n) = number of explants for each condition, * $p<0.01$.

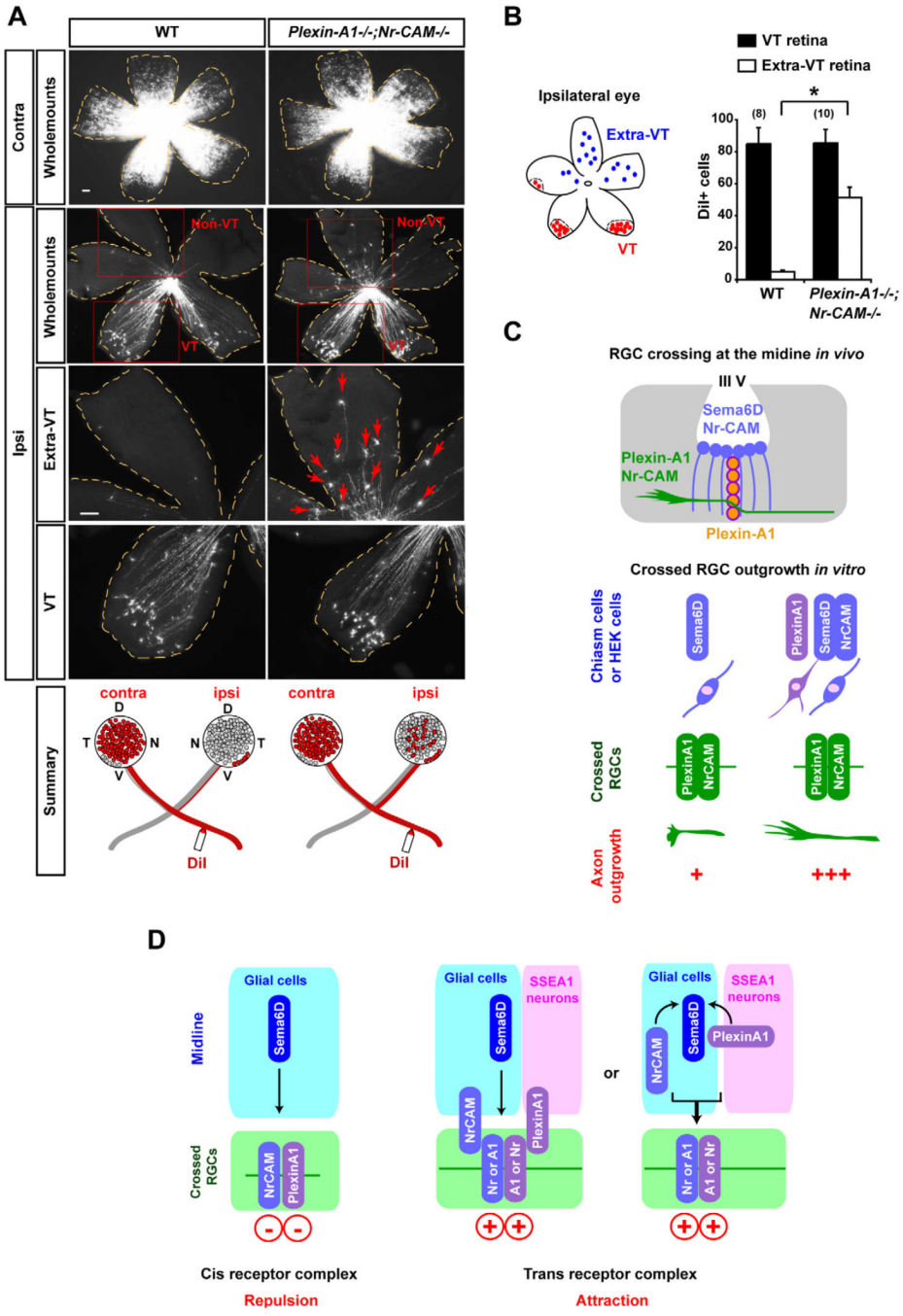

Figure 8. Non-VT RGCs are redirected ipsilaterally in *Plexin-A1*$^{-/-}$*;Nr-CAM*$^{-/-}$ mutants

(A) Representative E17.0 WT and *Plexin-A1*$^{-/-}$*;Nr-CAM*$^{-/-}$ mutant retina whole mounts, showing retrogradely labeled RGCs contralateral (Contra) or ipsilateral (Ipsi) to DiI application in the optic tract. While DiI^{+} RGCs are restricted to the VT crescent after ipsilateral DiI application to the optic tract in wild type retina, RGCs were also observed in non-VT retina after ipsilateral optic tract labeling in *Plexin-A1*$^{-/-}$*;Nr-CAM*$^{-/-}$ retina (arrows). (n ≥ 8 embryos for each condition). (B) Quantification of the ipsilateral projection from the VT and non-VT region in *Plexin-A1*$^{-/-}$*;Nr-CAM*$^{-/-}$ mutants. *Plexin-A1*$^{-/-}$*;Nr-CAM*$^{-/-}$ mutants show ~50 DiI^{+} RGCs in the non-VT region of ipsilateral retina, while WT display <5 DiI^{+} cells in non-VT regions. However, the number of DiI^{+} cells in VT regions

are not significantly different between WT and *Plexin-A1*$^{-/-}$*;Nr-CAM*$^{-/-}$ mutants. (C) Summary of interactions between Nr-CAM and Plexin-A1 on crossed RGCs and Sema6D substrates *in vitro*, and between Nr-CAM and Plexin-A1 on crossed RGCs and Nr-CAM/Sema6D (on midline radial glia) and Plexin-A1 (on SSEA-1^{+} neurons) in the chiasm *in vivo*. (D) Model of interactions between Nr-CAM and Plexin-A1 on crossed RGCs and Nr-CAM, Plexin-A1 and Sema6D on chiasm cells *in vivo*: changing the receptor complex in *cis* and reforming a receptor complex in *trans* between RGCs and chiasm cells implements RGC midline crossing. Scale bars, 100μm, (n) = number of explants for each condition, * $p<0.01$.